AEDC-TR-69-172

MEASUREMENTS AND CORRELATIONS OF TRANSITION REYNOLDS NUMBERS ON SHARP SLENDER CONES AT HIGH SPEEDS

S. R. Pate

ARO, Inc.

December 1969

VON KÁRMÁN GAS DYNAMICS FACILITY
ARNOLD ENGINEERING DEVELOPMENT CENTER
AIR FORCE SYSTEMS COMMAND
ARNOLD AIR FORCE STATION, TENNESSEE

NOTICES

When U. S. Government drawings specifications, or other data are used for any purpose other than a definitely related Government procurement operation, the Government thereby incurs no responsibility nor any obligation whatsoever, and the fact that the Government may have formulated, furnished, or in any way supplied the said drawings, specifications, or other data, is not to be regarded by implication or otherwise, or in any manner licensing the holder or any other person or corporation, or conveying any rights or permission to manufacture, use, or sell any patented invention that may in any way be related thereto.

Qualified users may obtain copies of this report from the Defense Documentation Center.

References to named commercial products in this report are not to be considered in any sense as an endorsement of the product by the United States Air Force or the Government.

MEASUREMENTS AND CORRELATIONS OF TRANSITION REYNOLDS NUMBERS ON SHARP SLENDER CONES AT HIGH SPEEDS

S. R. Pate
ARO, Inc.

FOREWORD

The work reported herein was sponsored by Headquarters, Arnold Engineering Development Center (AEDC), Air Force Systems Command (AFSC), in support of Project 8953, Task 03, Program Element 62201F.

The results of the research presented were obtained by ARO, Inc. (a subsidiary of Sverdrup & Parcel and Associates, Inc.), contract operator of AEDC, AFSC, Arnold Air Force Station, Tennessee, under contract F40600-69-C-0001. This report contains experimental data obtained during the period July 30 to September 26, 1968, under ARO Project No. VT0849, and the manuscript was submitted for publication on July 8, 1969.

This technical report has been reviewed and is approved.

Eugene C. Fletcher
Lt Colonel, USAF
AF Representative, VKF
Directorate of Test

Roy R. Croy, Jr.
Colonel, USAF
Director of Test

ABSTRACT

An experimental investigation of laminar boundary-layer transition on a sharp, 10-deg total-angle, insulated cone at zero yaw was conducted in the AEDC-VKF 12- and 40-in. supersonic wind tunnels at free-stream Mach numbers from 3 to 6. This research was directed toward defining the relationship between the aerodynamic noise disturbances and boundary-layer transition Reynolds numbers $(Re_t)_\delta$ in high-speed wind tunnels and has extended previously published planar results to include axisymmetric models. A significant increase in $(Re_t)_\delta$ with increasing tunnel size (similar to the planar results) is shown to exist. Sharp cone transition Reynolds numbers from ten facilities (12- to 54-in.) for free-stream Mach numbers from 3 to 14 and a unit Reynolds number per inch range from 0.1×10^6 to 1.2×10^6 have been correlated using aerodynamic-noise-transition parameters. A quantitative correlation of the ratio between cone and planar $(Re_t)_\delta$ values has been developed which demonstrates a strong Mach number dependence and also indicates a variation with tunnel size and unit Reynolds number.

CONTENTS

APPENDIXES

I. ILLUSTRATIONS

Figure

NOMENCLATURE

b	Model nose bluntness, in.
C_F	Mean turbulent skin friction coefficient
c	Tunnel test section circumference, in.
c_1	Tunnel test section circumference of 12- by 12-in. tunnel (c_1 = 48 in.)
ℓ_m	Axial distance from tunnel throat to model nose, in.

ℓ_r	Axial distance from tunnel throat to wall boundary-layer rake, in.
M	Mach number
p	Surface probe pitot pressure, psia
p_c	Cone surface static pressure, psia
p_o	Tunnel stilling chamber pressure, psia
p_o'	Total pressure downstream of a normal shock wave at free-stream conditions, psia
$\tilde{p}$	Root-mean-square of pressure fluctuation, psia
p_∞	Free-stream static pressure, psia
q_∞	Free-stream dynamic pressure, psia
$\dot{q}$	Heat-transfer rate, Btu/ft^2-sec
$(Re_t)_\delta$	Transition Reynolds number (based on local conditions), $(Re_t)_\delta = (Re/in.)_\delta \, x_t$
Re_δ or $(Re/in.)_\delta$	Inviscid flow local surface unit Reynolds number per inch, U_δ/ν_δ
Re_∞ or $(Re/in.)_\infty$	Free-stream Reynolds number per inch, U_∞/ν_δ
T	Static temperature, °R or °F
T_o	Tunnel stilling chamber total temperature, °R or °F
U	Velocity, ft/sec
x	Surface distance measured from cone apex, in.
x_t	Surface distance location of boundary-layer transition, in.
δ^*	Boundary-layer displacement thickness (tunnel wall), in.
θ_c	Cone half-angle, deg
μ	Absolute viscosity, $lb\text{-}sec/ft^2$
ν	Kinematic viscosity, in.-ft/sec

SUBSCRIPTS

aw	Adiabatic wall
c	Cone configuration

planar	Two-dimensional configuration, either hollow cylinder or flat plate
w	Wall
δ	Local inviscid flow properties
∞	Free-stream

SECTION I
INTRODUCTION

Whenever theoretical analyses for a particularly difficult, but equally important, physical phenomenon are known to be inadequate then solutions must, from necessity, be provided by experimental and empirical results. For over six decades the laminar boundary-layer transition process has defied the development of a successful theoretical analysis. Consequently, the bulk of the knowledge accumulated to date on this very complex fluid flow phenomenon has relied almost entirely on experimental data. Unfortunately, however, as experimentalists continue to gather transition data — to advance the state of the art and to meet the demands dictated by high performance reentry vehicles and supersonic-hypersonic cruise aircraft — it is becoming more evident that the transition process (as was the case with the now historic stability experiments of Ref. 1) is critically dependent, even at supersonic-hypersonic Mach numbers, on the free-stream disturbance modes present in conventional experimental facilities.

Facility-generated disturbances (primarily vorticity) present in subsonic and low supersonic ($M_\infty \leq 3$) wind tunnels have long been recognized to have a significant and adverse effect on transition, Refs. 1 through 7. However, for lack of evidence it has been the policy of most transition investigators to assume that the disturbance modes present at higher Mach numbers ($M_\infty \geq 3$) (primarily radiated sound or aerodynamic noise) had negligible effects on the location of transition and on the development of the transition process.

However, recent experimental transition research by Pate and Schueler, Refs. 8 and 9, has shown, conclusively, the severe, adverse effect that the aerodynamic noise which radiates from the turbulent boundary layer on the walls of supersonic and hypersonic tunnels will have on transition. These studies have provided an extensive and unique aerodynamic-noise-transition Reynolds number correlation of high-speed ($3 \leq M_\infty \leq 8$) wind tunnel $(Re_t)_\delta$ data from many different facilities. The intensity of the radiated noise as reported in Refs. 8 and 9 was related to the tunnel size, tunnel wall boundary-layer state (laminar, transitional, or turbulent), tunnel unit Reynolds number, and tunnel Mach number.

Over the years, experimentalists have attempted to establish a valid relationship between cone and flat plate transition Reynolds numbers. Perhaps the most significant results to date in this area were those reported in Refs. 10 and 11. From a qualitative comparison of $(Re_t)_\delta$ data obtained on axisymmetric and planar models from several sources and several different wind tunnels, Potter and Whitfield, Ref. 10, observed

that the $(Re_t)_\delta$ ratio (cone to planar) appeared to decrease from a value of approximately three at $M_\delta = 3$ to about one near $M_\delta = 8$. However, more recently in Ref. 11, Whitfield and Iannuzzi concluded that attempts at direct comparison of cone and planar $(Re_t)_\delta$ data from various high-speed facilities must now be viewed with reservation and that cone-planar $(Re_t)_\delta$ ratio results cannot be clearly established from presently available experimental data. Their conclusions were based primarily on the recent transition studies of Pate and Schueler, Refs. 8 and 9. Therefore, evidence to date appears to indicate that the free-stream disturbances present in high-speed test facilities are also masking the factor of three difference between cone and flat plate $(Re_t)_\delta$ values that have been reported experimentally and implied by many investigators using the theoretical analysis of Tetervin in Ref. 12.

The purpose of this research was to extend the investigation of tunnel aerodynamic noise effects on transition to include axisymmetric models. Slender cone models have been tested at $3 \leq M_\infty \leq 6$ to determine if cone transition Reynolds numbers varied appreciably with the tunnel size and to establish if an aerodynamic-noise-transition correlation similar to the planar results of Refs. 8 and 9 could be developed.

These transition studies, conducted in the Tunnels A and D (Gas Dynamic Wind Tunnels, Supersonic (A) and (D), respectively), have also provided new information on the relation between cone and flat plate (planar) transition Reynolds numbers obtained in high-speed ($3 \leq M_\infty \leq 8$), conventional wind tunnels.

SECTION II
EXPERIMENTAL CONDITIONS

2.1 WIND TUNNEL FACILITIES

New experimental data included in this report were obtained at the Arnold Engineering Development Center (AEDC) in the von Kármán Gas Dynamics Facility (VKF), supersonic Tunnels A and D.

2.1.1 Tunnel D

Tunnel D is an intermittent, variable density wind tunnel with a manually adjusted, flexible-plate-type nozzle and a 12- by 12-in. test section. The tunnel operates at Mach numbers from 1.5 to 5 at stagnation pressures from about 5 to 60 psia, respectively, and at average stagnation temperatures of about 70°F.

2.1.2 Tunnel A

Tunnel A is a continuous, closed-circuit, variable density wind tunnel with an automatically driven, flexible-plate-type nozzle and a 40- by 40-in. test section. The tunnel operates at Mach numbers from 1.5 to 6 at maximum stagnation pressures from 29 to 200 psia, respectively, and stagnation temperatures up to 290°F (M_∞ = 6). Minimum operating pressures range from about one-tenth to one-twentieth of the maximum pressures.

2.2 TRANSITION MODELS AND APPARATUS

The transition model, Figs. 1 and 2 (Appendix I), was a 10-deg total-angle, stainless steel cone equipped with a tool steel nose section. The model had a surface finish of approximately 10 μin. and a tip bluntness (b) between 0.005 and 0.006 in. The Tunnel D model consisted of the nose and center section as shown in Fig. 1. The Tunnel A model was obtained by adding an aft section as shown in Figs. 1 and 2. In order to maintain a near-perfect joint between the sections, the model surface was refinished after attaching each model section.

A remotely controlled, electrically driven, surface pitot probe (tip geometry illustrated in Fig. 1a) as shown in Figs. 1b and 2 provided a continuous trace of the probe pressure on an X-Y plotter from which the location of transition was determined.

Schlieren and shadowgraph photographic systems were used as a secondary method for detecting the location of transition in Tunnels D and A, respectively.

A 1/4-in.-diam, flush-mounted surface microphone having a frequency response from 0 to 30 kHz and a dynamic response from 70 to 180 db was also used to measure the model surface pressure fluctuations in the laminar, transitional, and turbulent flow regimes and to determine the location of transition.

SECTION III
INVISCID FLOW CONE PROPERTIES

The unit Reynolds number ratios at the surface of sharp, unyawed cones, assuming inviscid flow properties, have been calculated and the results are presented in Fig. 3. The justification for presenting these

results was precipitated by the fact that in reviewing published transition results it became apparent that inconsistencies existed in the calculation of tunnel unit Reynolds numbers and more often for cone surface values. These differences were traceable primarily to the different viscosity relationships used. Therefore, the surface Reynolds number ratios assuming inviscid flow over sharp, unyawed cones were calculated using three different methods.

1. Using the linear viscosity law ($\mu \approx T$) which is valid for temperatures below approximately 216°R.

$$\left[\frac{(Re_\delta)_c}{Re_\infty}\right]_{\text{linear law}} = \frac{p_c}{p_\infty}\frac{M_c}{M_\infty}\left(\frac{T_\infty}{T_c}\right)^{1.5} \tag{1}$$

2. Using Sutherland's viscosity law which is valid for temperatures above approximately 216°R.

$$\left[\frac{(Re_\delta)_c}{Re_\infty}\right]_{\text{Sutherland}} = \frac{p_c}{p_\infty}\frac{M_c}{M_\infty}\left(\frac{T_\infty}{T_c}\right)^{2}\left(\frac{T_c + 198.6}{T_\infty + 198.6}\right) \tag{2}$$

3. Using a combination of the linear and Sutherland viscosity laws

$$\left[\frac{(Re_\delta)_c}{Re_\infty}\right]_{\substack{\text{linear} \\ \text{plus Sutherland}}} = \frac{p_c}{p_\infty}\frac{M_c}{M_\infty}\left(\frac{T_\infty}{T_c}\right)^{1/2}\frac{\mu_\infty}{\mu_c} \tag{3}$$

for $T \leq 215°R$, $(\mu)_{\text{linear}} = (0.0805 \times 10^{-8})(T)$, lb-sec/ft^2

$T \geq 216°R$, $(\mu)_{\text{Sutherland}} = \dfrac{2.270 \times (T)^{1.5}}{198.6 + T} \times 10^{-8}$, lb-sec/ft^2

Equation (3) combines the two viscosity laws and thus provides the more general method for calculating the Reynolds number ratio. A combination of the viscosity laws allows the free-stream viscosity to be determined using the linear law and the cone surface value to be evaluated using the Sutherland law which is often the condition existing in wind tunnels at high supersonic and hypersonic Mach numbers.

Figure 3a presents the Reynolds number ratios for M_∞ = 2, 5, and 12 and cone half-angles (θ_c) from 0 to 35 deg. As clearly evident, the three methods can produce significant differences depending on the combined effects of cone angle and flow conditions.

A family of Reynolds number ratios calculated using Eq. (3) is shown in Fig. 3b. It may be noted that the ratios are temperature dependent at flow conditions where Sutherland's viscosity law was applicable. The temperatures (T_0) were selected to correspond to the range of total temperatures usually available in wind tunnels.

All of the transition Reynolds numbers presented in this report (including data from other sources) were calculated using Eq. (3) or were obtained from Fig. 3b.

SECTION IV
BASIC TRANSITION RESULTS

4.1 METHODS OF DETECTION

A surface pressure probe, microphone, and photography were used to detect transition.

4.1.1 Surface Probe

Typical surface probe transition profiles obtained in Tunnels D and A are presented in Figs. 4 and 5 for several Mach numbers and unit Reynolds numbers. Unless otherwise specified, the location of transition used in this study is defined as the peak in the pitot pressure profile as illustrated in Figs. 4 and 5. This method of transition detection is generally accepted as being near the end of the transition region (Refs. 13 and 14) and has been established as one of the more repeatable and reliable methods of selecting a particular and finite location of transition.

4.1.2 Microphone

Pressure fluctuation profiles obtained with the flush-mounted 1/4-in.-diam surface microphone are shown in Fig. 6. The sharp apex in the pressure profile was defined as the indication of transition at the microphone location. The transition Reynolds number, based on this definition, is compared to the pitot probe values in subsequent figures. It is of interest to note the similarity between the root-mean-square (rms) profiles and other measurements of the transition region, e.g., the surface probe (Figs. 4 and 5), heat-transfer rates (Refs. 15 and 16), and heat-transfer fluctuations (Ref. 17). Additional information on the spectral distribution of the pressure fluctuations in the laminar, transitional, and turbulent boundary layers on this configuration and a description of the microphone instrumentation and recording procedures are reported in Ref. 18.

4.1.3 Photographic Observations

The location of transition as determined from schlieren and shadowgraph photographs was selected at the body station where the boundary layer had developed into what appeared visually to be fully turbulent flow. This location of transition provided $(Re_t)_\delta$ values, in general, about 10 to 20 percent lower than $(Re_t)_\delta$ results obtained from the surface probe peak pressure locations. Any burst, ripples, or rope effects that were observable upstream of the fully developed turbulent location were ignored in the selection of x_t. The transition values presented represent an average x_t value determined from approximately four different photographs.

4.2 TRANSITION REYNOLDS NUMBERS

As stated in Section I, one of the primary objectives of this research was to provide sharp cone $(Re_t)_\delta$ data suitable for direct comparison with existing two-dimensional hollow cylinder data reported in Refs. 8, 9, and 13. To maintain as nearly identical free-stream flow disturbances as possible, the cone was positioned in the tunnel very near the previous hollow cylinder locations and the experiments were conducted at equivalent free-stream Mach number and unit Reynolds number values.

The transition Reynolds number results for Tunnels D and A are presented in Figs. 7 and 8 (see also Tables I and II, Appendix II) and appear quite normal in that they exhibit the usual increase in $(Re_t)_\delta$ with increasing $(Re/in.)_\delta$ and the photographic values are about 10 to 20 percent lower than the surface probe values. Although the microphone results were limited to two data points, the peak in the pressure fluctuation profile appears to provide $(Re_t)_\delta$ values consistent with the surface probe and photographic values.

One of the known (but sometimes forgotten) variables that can affect the transition location is the dew point (temperature at standard atmospheric pressure at which water condensation occurs), Ref. 19. In Tunnel D the dew point was sufficiently low (< 0°F) at all Mach numbers not to affect the x_t locations. Also, in Tunnel A the dew point was sufficiently low[1] at all Mach numbers except for the lower unit Reynolds numbers (subatmospheric pressure levels) at $M_\infty = 3$, as illustrated in Fig. 8a. Therefore,

---

[1]The relatively high dew point existing in the $M_\infty = 3$ data reflects facility limitations existing on that particular date and does not necessarily represent standard test conditions.

a suggested $(Re_t)_\delta$ trend as indicated by the dashed line has been included in Fig. 8a for $M_\infty = 3$.

SECTION V
TRANSITION CORRELATION

The primary objective of this research was to determine if sharp cone transition Reynolds numbers varied with tunnel size in accordance with the previously published planar results and to establish if the $(Re_t)_\delta$ values could be correlated using the aerodynamic-noise-transition parameters developed by Pate and Schueler, Refs. 8 and 9.

There was a large increase in the cone $(Re_t)_\delta$ values from Tunnels D and A at all test Mach numbers as can be readily determined by a comparison of the data in Figs. 7 and 8. Figure 9 presents a direct comparison of the $M_\infty = 4$ cone $(Re_t)_\delta$ data from Tunnels D and A. The large increase in $(Re_t)_\delta$ with increasing tunnel size is clearly evident and is very similar to the planar results from Refs. 8 or 9 which are included for a quantitative comparison. The increase in $(Re_t)_\delta$ with increasing tunnel size is explained by a decrease in the aerodynamic-noise intensities that radiate from the turbulent boundary layer on the tunnel walls. A more comprehensive discussion of this type of disturbance mode and the aerodynamic-noise-transition correlation parameters (δ^*, C_F, and c) is given in Refs. 8 and 9.

Transition Reynolds numbers on sharp slender cones were correlated as shown in Fig. 10 using the aerodynamic-noise-transition parameters developed by Pate and Schueler in Refs. 8 and 9. Data used in the cone correlation were obtained not only from the present investigation, but from a total of ten sources representing ten different wind tunnel facilities. The data covered a free-stream Mach number range from 3 to 14, an $(Re/in.)_\infty$ range from 0.1×10^6 to 1.2×10^6, and test section sizes from 12 in. square to 54 in. in diameter. Specific information on the range of test conditions and pertinent information on model geometry are provided in Table III. Also included in Fig. 10 is the correlation of two-dimensional $(Re_t)_\delta$ data taken from Refs. 8 and 9. The $(Re_t)_\delta$ data obtained with detection methods other than a surface probe were adjusted in accordance with the findings of Refs. 13 and 14 as specified in Table III.

One factor that must be recognized in the correlation of cone data is the absence of a one-to-one relation or even a constant ratio between the free-stream and cone surface unit Reynolds numbers. If a series of cone angles had been selected which would have allowed a constant ratio of

certain cone to free-stream parameters - say the unit Reynolds number ratio - to have been maintained, then any relationship that might have existed between the strength of the cone bow shock wave and/or the receptivity of the cone laminar flow to the radiated noise levels after passage through the bow shock would possibly have remained more constant. Future investigations in these areas would, or course, be desirable. Notwithstanding these uncertainties, the cone $(Re_t)_\delta$ values are shown (Fig. 10) to correlate fairly well without exhibiting a significant dependence on the cone angle. It is perhaps of special interest to note that $(Re_t)_\delta$ data from the AEDC-VKF Hotshot Tunnel F (Gas Dynamic Wind Tunnel, Hypersonic (F)), although a little low, appear to correlate. In addition to the radiated sound disturbances that are presumed to be present in Tunnel F, there is also the likely possibility that significant free-stream entropy fluctuations (temperature spottiness) are also present. It would be expected that this additional disturbance mode would also have an adverse effect on $(Re_t)_\delta$.

An empirical equation for the two-dimensional planar correlation was reported in Refs. 8 and 9 to be

$$\left[(Re_t)_\delta\right]_{planar} = \frac{0.0141\,(C_F)^{-2.55}\left[0.56 + 0.44\left(\frac{c_1}{c}\right)\right]}{\sqrt{\frac{\delta^*}{c}}} \tag{4}$$

An empirical equation that fits the cone data fairly well can be written as

$$\left[(Re_t)_\delta\right]_{cone} = \frac{10.5\,(C_F)^{-1.66}\left[0.56 + 0.44\left(\frac{c_1}{c}\right)\right]}{\sqrt{\frac{\delta^*}{c}}} \tag{5}$$

There are several significant results (other than the basic correlation which was independent of Mach number and unit Reynolds number) to be deduced from Fig. 10.

First: The sharp cone and planar correlations appear to intersect at the low C_F values ($M_\infty \gtrsim 8$) and diverge as C_F increases ($M_\infty \to 3$). This trend implies that the ratio of cone to planar $(Re_t)_\delta$ values is dependent on Mach number, tunnel size, and unit Reynolds number. A detailed discussion on this subject is pursued in Section VII.

Second: A literal interpretation of the correlation suggests that Tunnel F planar $(Re_t)_\delta$ values would be larger than cone values. The validity of this inference will have to wait for experimental verification.

The average turbulent skin friction coefficients (C_F) used in the transition correlation were determined using Ref. 20, in conjunction with the tunnel free-stream Mach number and a length Reynolds number based on $(Re/in.)_\infty$ and the model axial location (ℓ_m) as measured from the tunnel throat. Information concerning the determination of the tunnel wall δ^* values is provided in Table III.

The reader should be aware that the $(Re_t)_\delta$ correlations presented in Fig. 10 are applicable only to wind tunnels having turbulent wall boundary layers. Consequently, the correlations cannot be used for evaluation of ballistic range or free-flight transition locations. Furthermore, the experimental data and correlations presented should not be used to reach conclusive decisions regarding the "true" Mach number and unit Reynolds number variations that may exist in a disturbance-free environment (either free-flight or experimental facility). However, it has been established that - at least in conventional supersonic and hypersonic wind tunnels - radiated noise is a major and perhaps dominating influence on the transition location and process.

SECTION VI
TUNNEL SIZE AND MACH NUMBER EFFECTS

Significant increases in planar transition Reynolds numbers with increasing tunnel size as a result of a decrease in the radiated aerodynamic noise were thoroughly documented by Pate and Schueler, Refs. 8 and 9. Cone $(Re_t)_\delta$ data obtained during the present investigation in Tunnels A and D demonstrated a similar increase with increasing tunnel size as was illustrated in Fig. 9.

A composite plot of data from the present study and several other sources is presented in Fig. 11. These results firmly establish the existence of a significant increase in cone and planar $(Re_t)_\delta$ values with increasing tunnel size. The data presented also clearly indicate that only by comparing data obtained in identical test environments can a valid and meaningful relationship between cone and planar $(Re_t)_\delta$ ratios be established.

Figure 11 also adds substantial support to the conclusion of Refs. 8 and 9 that the "true" Mach number effect on transition cannot be established from wind tunnel models exposed to aerodynamic noise. It is perhaps also of interest to note the difference in Mach number trends between the cone and planar $(Re_t)_\delta$ data which exists even when the fairing is based on data from tunnels of similar size.

The predicted $(Re_t)_\delta$ values obtained using Eqs. (4) and (5) are also included in this figure, and the agreement with the experimental data in both trends and levels is considered quite satisfactory.

Variations of transition with tunnel size are perhaps most strikingly demonstrated at $M_\infty = 3$ where the cone and planar data are presented for tunnels varying in size from 5 to 40 in. and from 1 to 16 ft, respectively.

Concerning Mach number effects, the reader is referred to the results obtained by Stainback at NASA-Langley (Ref. 21) which were represented and discussed in Refs. 8 and 9. These studies report that when the tunnel and cone local unit Reynolds number were held approximately constant and the cone local Mach number was varied from about 4 to 8 — by proper selection of cone angles — then the $(Re_t)_\delta$ values were independent of Mach number. These results are in agreement with the proposed aerodynamic-noise-transition relation and with the correlations presented in Fig. 10.

SECTION VII
AXISYMMETRIC AND PLANAR TRANSITION CORRELATION

Potter and Whitfield in Ref. 10 made a qualitative comparison of $(Re_t)_\delta$ data obtained on cones and planar bodies from several sources and observed that the ratio of $(Re_t)_{\delta,\,cone}/(Re_t)_{\delta,\,planar}$ appeared to decrease from a value of approximately 3 at $M_\infty \approx 3$ to a value of about 1.1 at $M_\infty \approx 8$. Based on the planar results of Pate and Schueler, Refs. 8 and 9, Whitfield and Iannuzzi in Ref. 11 concluded that attempts at comparison of $(Re_t)_\delta$ from various high-speed facilities as done in Ref. 10 must now be viewed with reservation, and the relationship between cone and planar $(Re_t)_\delta$ results could not be established from presently available data.

Therefore, one of the primary objectives of this research was to attempt to establish a quantitative correlation of sharp slender cones (axisymmetric) and flat plate-hollow cylinder (planar) transition Reynolds numbers at supersonic and hypersonic speeds.

Based on the results of Refs. 8 and 9, it was realized that a correlation was possible only if cone and flat plate data were obtained in the same test facility, under identical test conditions, using equivalent methods of transition detection. There are no available investigations of the receptivity of a laminar boundary layer to radiated noise. Consequently, it was necessary to obtain $(Re_t)_\delta$ data exposed to various intensity levels of radiated noise while continuing to maintain a constant free-steam unit

Reynolds number and Mach number if the cone-planar $(Re_t)_\delta$ relation was to be determined. This was accomplished by obtaining test data in significantly different-sized tunnels (VKF Tunnels A and D).

Presented in Fig. 12 is a correlation of cone and flat plate $(Re_t)_\delta$ data developed from the data obtained in this study and Refs. 8 and 9 (VKF Tunnels A and D) and data from three other test facilities. Based on the results of Refs. 8 and 9, it can be argued that there are various procedures that are available for reducing this type of data. The three procedures used are outlined in the legend of Fig. 12. The significant conclusions to be drawn from this figure are: (1) The $(Re_t)_\delta$ ratio appears to be about 2.2 to 2.5 at $M_\infty = 3$. (2) The trend decreases monotonically with increasing Mach number to a value of approximately 1.0 to 1.1 at $M_\infty = 8$. (3) Close inspection of these results at a given Mach number ($M_\infty = 3$ to 5) suggests a decrease in the $(Re_t)_\delta$ ratio with increasing tunnel size. This finding is in agreement with the correlation results presented in Fig. 10. (4) The $(Re_t)_\delta$ ratio is also slightly dependent on the method of analysis.

An empirical equation for the cone-planar $(Re_t)_\delta$ ratios can be obtained by ratioing Eqs. (4) and (5).

Then

$$\frac{(Re_t)_{\delta,\text{cone}}}{(Re_t)_{\delta,\text{planar}}} = \frac{\text{Eq. (5)}}{\text{Eq. (4)}} = 745\,(C_F)^{0.89} \tag{6}$$

Predicted transition ratios using Eq. (6) are presented in Fig. 13 for a large range of tunnel sizes, Mach numbers, and $(Re/in.)_\infty$ values. The experimental data for the 40- and 50-in. tunnels ($3 \leq M_\infty \leq 8$) are in good agreement with the empirically predicted ratios. The data also indicate, qualitatively at least, a decrease in the transition ratio with an increase in tunnel size.

Many investigators have referenced the analytical analysis of Tetervin, Ref. 12, when attempting to explain the cone-planar $(Re_t)_\delta$ ratios of approximately three that were observed experimentally. Therefore, it appears of interest to consider Tetervin's theoretical results (Refs. 12, 22, and 23) in some detail.

From Tetervin's theoretical analysis in Ref. 22

$$\frac{(Re_t)_{\delta,\text{ cone}}}{(Re_t)_{\delta,\text{ planar}}} = 1 + 2\,\frac{(Re_t)_{\delta,\text{ planar-minimum}}}{(Re_t)_{\delta\text{ planar}}} \tag{7}$$

The $(Re_t)_{\delta, \text{planar-minimum}}$ values represent the theoretical minimum transition Reynolds number that can occur on a flat plate, and these values are presented as a function of Mach number and model surface temperature in Ref. 22.

Tetervin's theoretical transition ratio (Eq. (7)) was derived using linear stability theory. As shown by Eq. (7) when $(Re_t)_{\delta, \text{planar}}$ is near the minimum possible value then the cone-planar ratio approaches a value of three. As $(Re_t)_{\delta, \text{planar}}$ moves farther downstream then Eq. (7) approaches a value of unity. The assumptions that must be applied to Tetervin's analysis are: (1) free-stream disturbances are nonexistent, or (2) the disturbances affect only the laminar region of instability upstream of the respective $(Re_t)_{\delta, \text{planar-minimum}}$ locations, or (3) the absorptivity characteristics of the laminar layers on both the cone and flat plate downstream of the $(x_t)_{\text{planar-minimum}}$ locations are identical. There are no available experimental supersonic data that comply with assumption No. 1, and with disturbances present there is no evidence to support assumptions (2) and (3). Nevertheless, it appears to be of interest to use Eq. (7) and the theoretical $(Re_t)_{\delta, \text{planar-minimum}}$ values of Ref. 22 in conjunction with the experimental $(Re_t)_{\delta\text{-planar}}$ values presented in Fig. 11 of this study to estimate a few cone-planar transition ratios. The results are listed in column six of Table IV.

An increased value for Eq. (7) can be obtained if experimentally measured minimum critical Reynolds number (Fig. 3 of Ref. 12, showing the stability data of Schubauer and Skramstad, Laufer and Vrebalovich, and Demetriades) is used instead of the theoretical estimates of Tetervin. Also the $(Re_t)_\delta$ values presented in Fig. 11 (and used in the previous evaluation of Eq. (7)) correspond to the maximum pitot probe pressure location which is on the order of a factor of two downstream of what one might consider as a "measurable" beginning of transition. Incorporating these adjustments into Eq. (7) produces the cone-planar ratios tabulated in column seven of Table IV.

For a factor of three to exist in the estimated cone-planar transition ratio at $M_\infty = 3$ would require, depending on the method of analysis, a two-dimensional $(Re_t)_{\delta, \text{planar}}$ value of 16,000 to 80,000. To the author's knowledge, these values are on the order of a factor of 10 to 50 below any published data. Therefore, it would seem that the cone to flat plate ratio of three quoted by many investigators as being theoretically predicted by Eq. (7) is perhaps without adequate foundation, and the apparent agreement with experimental data that appeared to exist is perhaps only fortuitous. Similarly, the decrease to approximately one exhibited by the experimental data in Figs. 12 and 13 as the Mach number approaches eight does not appear, based on the results in Table IV, to be explained by

Eq. (7). Based on the available information it is suggested that the absolute values produced by Eq. (7) are, at best, not adequate for accurate predictions or for laying a foundation for analyzing experimental transition results. However, it is of interest to note the trend predicted by Eq. (7) for a constant Mach number when the value of $(Re_t)_{\delta, \text{planar-minimum}}$ is assumed constant. The cone-planar $(Re_t)_\delta$ ratio as given by Eq. (7) is seen to decrease with increasing experimental $(Re_t)_{\delta\text{-planar}}$ values — which will occur with increasing tunnel size or increasing $(Re/in.)_\infty$ — and this trend is in agreement with the experimental results shown in Figs. 12 and 13.

SECTION VIII
COMPARISON OF TUNNEL AND RANGE RESULTS

Figure 14 presents a direct and quantitative comparison of transition data from sharp slender cones obtained in wind tunnels and an aeroballistic range, Ref. 24, at equivalent local Mach numbers using similar methods of detection. At a comparable $(Re/in.)_\delta$ value, these data suggest that the range $(Re_t)_\delta$ data are significantly lower than the tunnel results, even for the 12-in. tunnel.

One major nonsimilarity between the tunnel and range experimental conditions is in the surface temperature ratios. Transition reversals have been predicted theoretically, Ref. 25, and verified experimentally, Refs. 26 and 27, and possible transition reversals have been shown experimentally, Ref. 27. However, to the author's knowledge, there are no experimental data that show transition Reynolds number to decrease below the adiabatic wall value for any degree of surface cooling. Therefore, if comparisons could be made where the model wall to free-stream temperature ratios were comparable, then a larger difference between tunnel and range $(Re_t)_\delta$ data than suggested by Fig. 14 might exist.

One question that naturally arises is whether adverse environmental or model disturbances could be affecting the range results. Only additional and new experimental range data can answer this question. It is also of interest to note that the data in Fig. 14 indicate a significant difference between the tunnel and range Re_t versus $(Re/in.)_\delta$ slope. The significance of the unit Reynolds number effect evident in the range data and the results of preliminary investigations on range noise disturbances have been reported in Ref. 24.

SECTION IX
CONCLUDING REMARKS

The significant results obtained from this experimental research were:

1. Boundary-layer transition measurements made on a sharp, 10-deg total-angle cone in a 12- and 40-in. wind tunnel at Mach numbers from 3 to 4.5 have shown a significant increase in transition Reynolds numbers $(Re_t)_\delta$ with increasing tunnel size. These variations with tunnel size are in agreement with previously published planar results and provide additional confirmation of the severe adverse effect radiated aerodynamic noise has on transition. The variation of $(Re_t)_\delta$ with tunnel size is explained by the aerodynamic noise that radiates from the tunnel wall turbulent boundary layer.
2. A correlation of transition Reynolds numbers $(Re_t)_\delta$ data from ten different wind tunnel facilities covering a Mach number range from 3 to 14, a unit Reynolds number per inch range from 0.1×10^6 to 1.2×10^6 and tunnel test section sizes from 12 in. square to 54 in. in diameter was developed. The correlation was independent of Mach number and unit Reynolds number and dependent only on the aerodynamic-noise parameters established by Pate and Schueler for planar $(Re_t)_\delta$ data.
3. These axisymmetric $(Re_t)_\delta$ data and the resulting aerodynamic-noise-transition correlation provide additional confirmation to the earlier suggestions by Pate and Schueler that extreme caution must be exercised when attempting to establish so-called "true" Mach number and unit Reynolds number trends from transition data obtained in conventional supersonic and hypersonic tunnels because of the strong adverse effect of aerodynamic-noise disturbances.
4. A quantitative correlation of cone to planar transition Reynolds number ratios was developed. The data correlation and an empirical equation (based on the aerodynamic-noise-transition correlation) show a monotonic decrease in the transition ratios with increasing Mach number. A dependence on tunnel size and unit Reynolds number, in addition to the Mach number trend, is also indicated.

5. The theoretical analysis of cone-planar transition ratios developed by Tetervin and often quoted by experimentalists as predicting a factor of three to exist, does not appear to provide a satisfactory explanation of the results presented in this report.

6. Wind tunnel $(Re_t)_\delta$ results are shown to be significantly higher than ballistic range data at $M_\delta = 4.3$ and $(Re/in.)_\delta \approx 0.6 \times 10^6$. Additional experimental testing is required to explain this apparent anomaly.

REFERENCES

1. Schubauer, G. B. and Skramstad, H. K. "Laminar-Boundary-Layer Oscillations and Transition on a Flat Plate." NACA Report No. 909, 1948.

2. van Driest, E. R. and Blumer, C. B. "Boundary Layer Transition: Free-Stream Turbulence and Pressure Gradient Effect." AIAA Journal, Vol. I, No. 6, June 1963, pp. 1303-1306.

3. Czarnecki, K. R. and Sinclair, Archibald R. "Factors Affecting Transition at Supersonic Speeds." NACA RM L53118a, November 1953.

4. Kovasznay, Leslie, S. G. "Turbulence in Supersonic Flow." Journal of the Aeronautical Sciences, Vol. 20, No. 10, 1953, pp. 657-674, 682.

5. van Driest, E. R. and Boison, J. Christopher. "Experiments on Boundary-Layer Transition at Supersonic Speeds." Journal of the Aeronautical Sciences, Vol. 24, No. 12, December 1957, pp. 885-899.

6. Laufer, John. "Aerodynamic Noise in Supersonic Wind Tunnels." Journal of the Aerospace Sciences, Vol. 28, 1961, pp. 685-692.

7. Morkovin, M. U. "On Supersonic Wind Tunnels with Low Free-Stream Disturbances." Journal of Applied Mechanics, Paper No. 59-APM-10, Vol. 26, 1959, pp. 319-324.

8. Pate, S. R. and Schueler, C. J. "Radiated Aerodynamic Noise Effects on Boundary Layer Transition in Supersonic and Hypersonic Wind Tunnels." AIAA Journal, Vol. 7, No. 3, March 1969, pp. 450-457.

9. Pate, S. R. and Schueler, C. J. "Effects of Radiated Aerodynamic Noise on Model Boundary Layer Transition in Supersonic and Hypersonic Wind Tunnels." AEDC-TR-67-236 (AD666644), March 1968.

10 Potter, J. Leith and Whitfield, Jack D. "Boundary-Layer Transition under Hypersonic Conditions." AEDC-TR-65-99 (AD462716), May 1965, also AGARD Specialists' Meeting on Recent Developments in Boundary-Layer Research, May 1965, AGARDograph 97, Part III.

11. Whitfield, Jack D. and Iannuzzi, F. A. "Experiments on Roughness Effects on Boundary-Layer Transition up to Mach 16." AEDC-TR-68-261 (AD680398), January 1969, also AIAA Paper No. 68-377, AIAA Journal, Vol. 7, No. 3, March 1969, pp. 465-470.

12. Tetervin, N. "An Estimate of the Minimum Reynolds Number for Transition from Laminar to Turbulent Boundary Layer Flow by Means of Energy Considerations." U. S. Naval Ordnance Laboratory, NAVORD Report 6854 (AD437345), January 1961.

13. Potter, J. Leith and Whitfield, Jack D. "Effects of Unit Reynolds Number, Nose Bluntness, and Roughness on Boundary-Layer Transition." AEDC-TR-60-5 (AD234478), March 1960.

14. Whitfield, Jack D. and Potter, J. Leith. "The Influence of Slight Leading-Edge Bluntness on Boundary-Layer Transition at a Mach Number of Eight." AEDC-TDR-64-18 (AD431533), March 1964.

15. Brinich, Paul F. and Sands, Norman. "Effect of Bluntness on Transition for a Cone and a Hollow Cylinder at Mach 3.1." NACA TN 3979, May 1957.

16. Brinich, Paul F. "Recovery Temperature, Transition, and Heat-Transfer Measurements at Mach 5." NASA TN D-1047, August 1961.

17. Owen, F. K. "Transition Experiments on a Flat Plate at Subsonic and Supersonic Speeds." AIAA Paper No. 69-9, Presented at AIAA 7th Aerospace Sciences Meeting, January 1969.

18. Pate, S. R. and Brown, M. D. "Acoustic Measurements in Supersonic Transitional Boundary Layers." AEDC-TR-69-182, October 1969, also ISA Paper No. 1.3.1, Presented at the 15th National Instrument Society of America (ISA) Aerospace Symposium, May 5-7, 1969, Las Vegas, Nevada.

19. Laufer, John and Marte, Jack E. "Results and Critical Discussion of Transition-Reynolds-Number Measurements on Insulated Cones and Flat Plates in Supersonic Wind Tunnels." JPL Report No. 20-96, November 1955.

20. van Driest, E. R. "Turbulent Boundary Layer in Compressible Fluids." Journal of the Aeronautical Sciences, Vol. 18, No. 3, March 1951, pp. 145-160, 216.

21. Stainback, Calvin P. "Some Effects of Roughness and Variable Entropy on Transition at a Mach Number of 8." AIAA Paper No. 67-132, Presented at AIAA 5th Aerospace Sciences Meeting, New York, New York, 1967.

22. Tetervin, Neal. "An Estimate of the Minimum Reynolds Number for Transition from Laminar to Turbulent Flow by Means of Energy Considerations." Journal of the Aerospace Sciences, February 1961, pp. 160-161.

23. Tetervin, Neal. "A Discussion of Cone and Flat-Plate Reynolds Numbers for Equal Ratios of the Laminar Shear to the Shear Caused by Small Velocity Fluctuations in a Laminar Boundary Layer." NACA TN 4078, August 1957.

24. Potter, J. Leith. "Observations on the Influence of Ambient Pressure on Boundary Layer Transition." AIAA Journal, Vol. 6, No. 10, October 1968, pp. 1907-1911.

25. Reshotko, E. "Transition Reversal and Tollmien-Schlichting Instability." Physics of Fluids, Vol. 6, No. 3, 1963, pp. 335-342.

26. Wisniewski, R. J. and Jack, J. R. "Recent Studies on the Effect of Cooling on Boundary-Layer Transition at Mach 4." Journal of the Aerospace Sciences, Vol. 28, 1961, p. 250.

27. Richards, B. E. and Stollery, J. L. "Further Experiments on Transition Reversal at Hypersonic Speeds." AIAA Journal, Vol. 4, No. 12, December 1966, pp. 2224-2226.

28. Bell, D. R. "Boundary-Layer Characteristics at Mach Numbers 2 through 5 in the Test Section of the 12-Inch Supersonic Tunnel (D)." AEDC-TDR-63-192 (AD418711), September 1963.

29. Jones, Jerry. "An Investigation of the Boundary-Layer Characteristics in the Test Section of a 40- by 40-Inch Supersonic Tunnel." AEDC-TN-60-189 (AD245362), October 1960.

30. Sivells, J. C. and Payne, R. G. "A Method of Calculating Turbulent-Boundary-Layer Growth at Hypersonic Mach Numbers." AEDC-TR-59-3 (AD208774), February 1959.

31. Dayman, Bain, Jr. "Comparison of Calculated with Measured Boundary-Layer Thicknesses on the Curved Walls of the JPL 20-in. Supersonic Wind Tunnel Two-Dimensional Nozzle." JPL Technical Report No. 32-349, March 1963.

32. Edenfield, E. E. "Contoured Nozzle Design and Evaluation for Hotshot Wind Tunnels." AIAA Paper No. 68-369, Presented at 3rd AIAA Testing Conference, April 1968.

33. McCauley, W. D., Saydah, A. R. and Bueche, J. F. "Effect of Spherical Roughness on Hypersonic Boundary-Layer Transition." AIAA Journal, Vol. 4, No. 12, December 1966, pp. 2142-2148.

34. Everhart, Philip E. and Hamilton, H. Harris. "Experimental Investigation of Boundary-Layer Transition on a Cooled 7.5-deg Total-Angle Cone at Mach 10." NASA TN D-4188, October 1967.

35. van Driest, E. R. and McCauley, W. D. "The Effect of Controlled Three-Dimensional Roughness on Boundary-Layer Transition at Supersonic Speeds." Journal of the Aero/Space Sciences, Vol. 27, April 1960, pp. 261 to 271.

36. Rogers, Ruth H. "Boundary Layer Development in Supersonic Shear Flow." AGARD Report 269, April 1960.

37. Sanator, R. J. and DeCarlo, J. P. "Hypersonic Boundary Layer Transition Data for a Cold Wall Slender Cone." AIAA Journal, Vol. 3, No. 4, April 1965, pp. 758-760.

38. Nagel, A. L., Savage, R. T. and Wanne., R. "Investigation of Boundary Layer Transition in Hypersonic Flow at Angle of Attack." AFFDL-TR-66-122, June 1966.

39. Deem, Ralph E. and Murphy, James S. "Flat Plate Boundary Layer Transition at Hypersonic Speeds." AIAA Paper No. 65-128, Presented at 2nd Aerospace Sciences Meeting, New York, New York, 1965.

APPENDIXES

I. ILLUSTRATIONS
II. TABLES

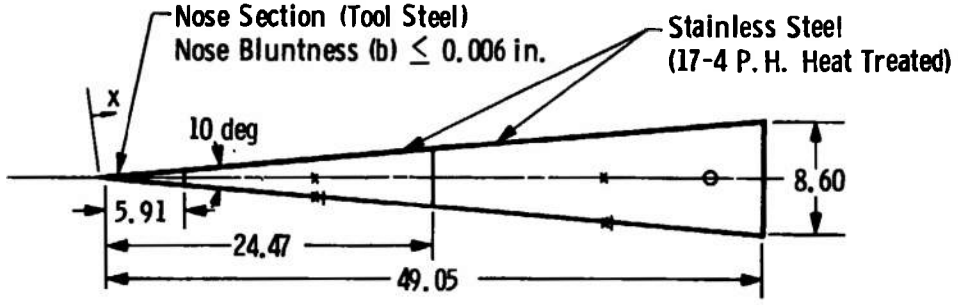

All Dimensions in Inches
Tunnel D Model Configuration ℓ = 24.47 in.
Tunnel A Model Configuration ℓ = 49.05 in.
Model Surface Finish 5 to 10 Microinches

Model Instrumentation			
Sym	Type	Quantity	Surface Location x, in.
x	Pressure Orifice, (0.020-in. -diam)	4	15.59, 37.26 (90 deg Apart)
I	Thermocouple	2	16.08, 37.76
o	Microphone	1	45.51

a. Model Details

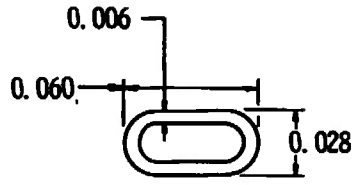

Probe A
(Used in Tunnels D and A)

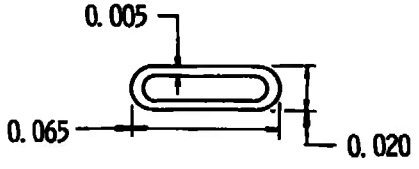

Probe B
(Used in Tunnel A Only)

PROBE DETAILS

Fig. 1 Model Geometry

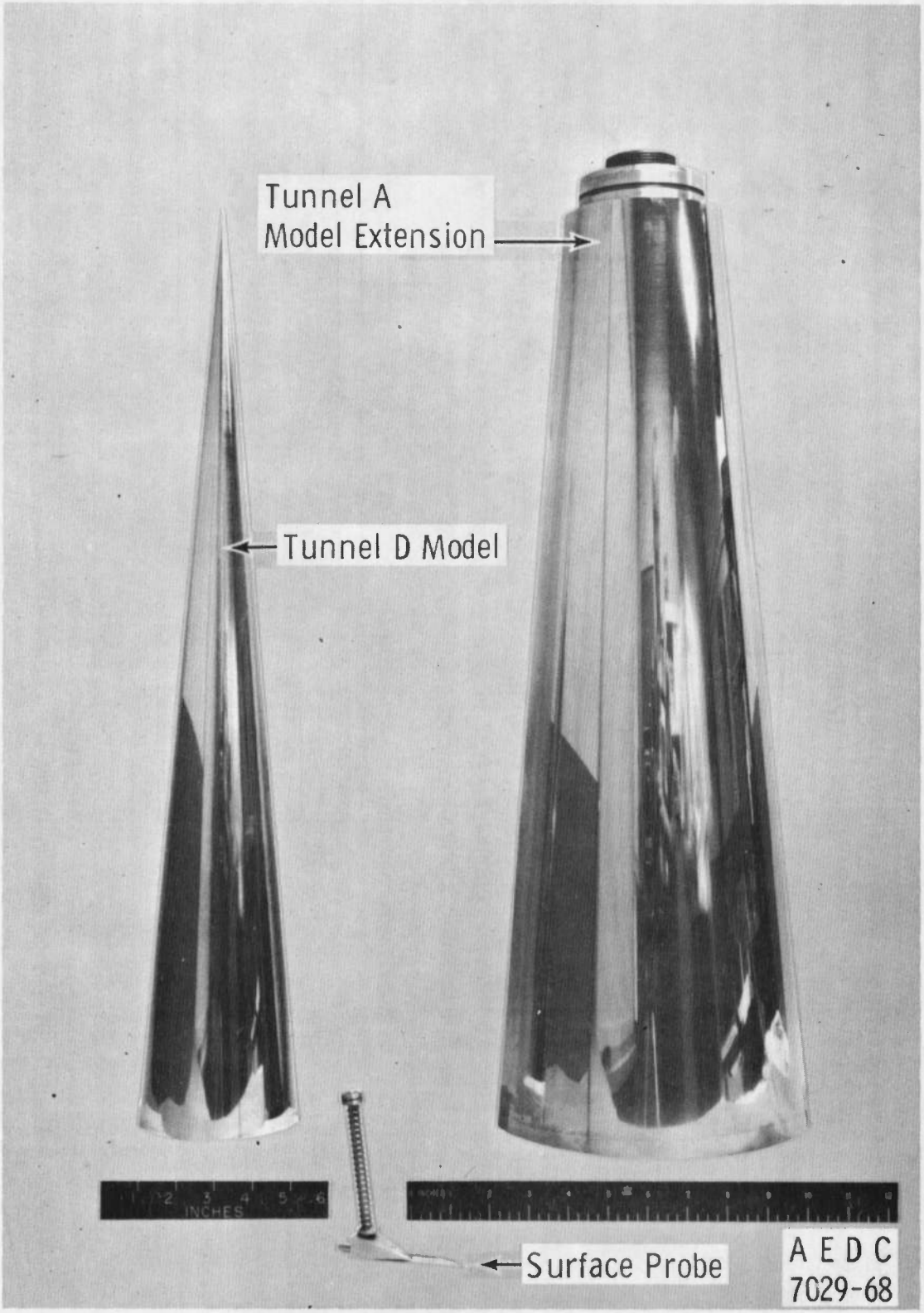

b. Photograph of Model Components
Fig. 1 Concluded

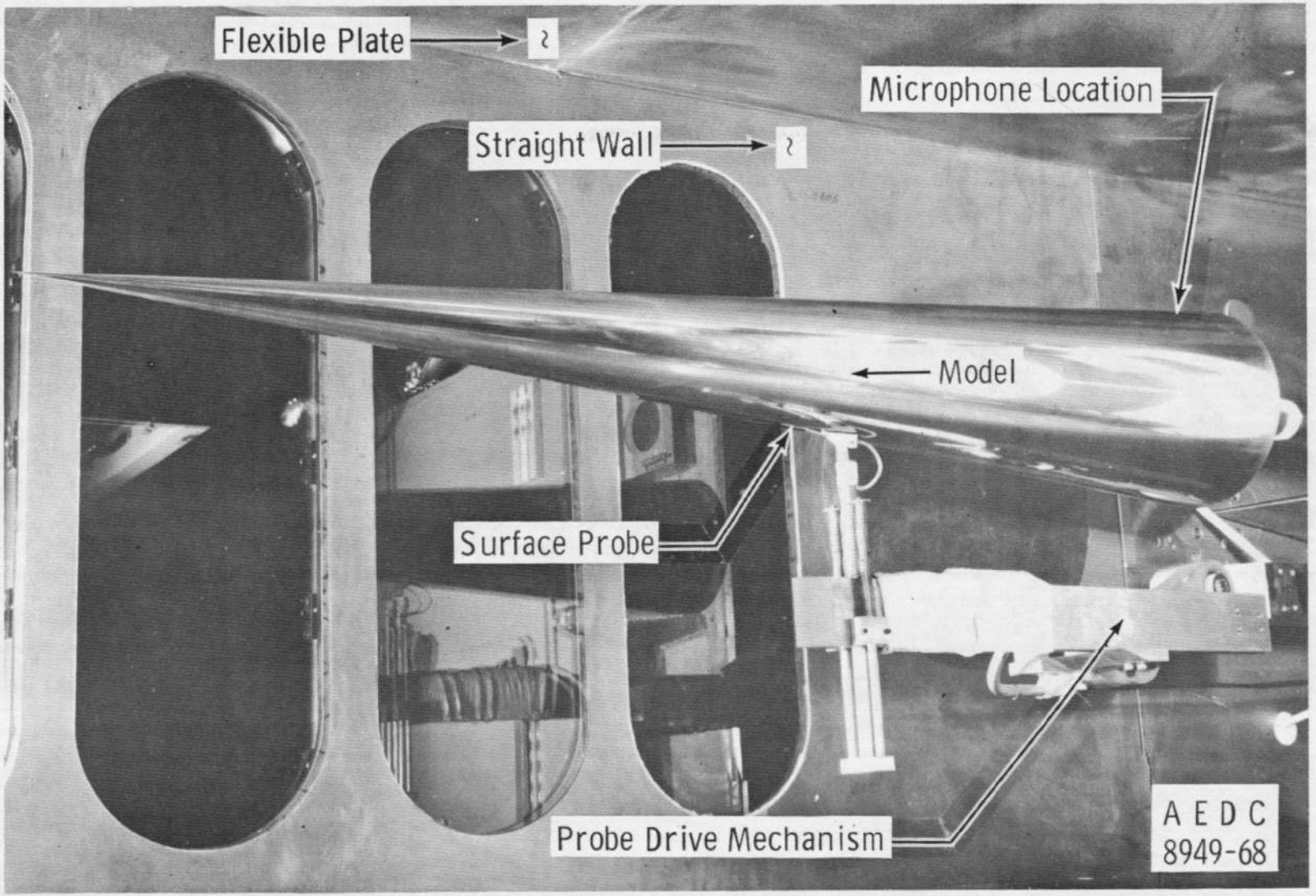

Fig. 2 Tunnel A Cone Model Installation

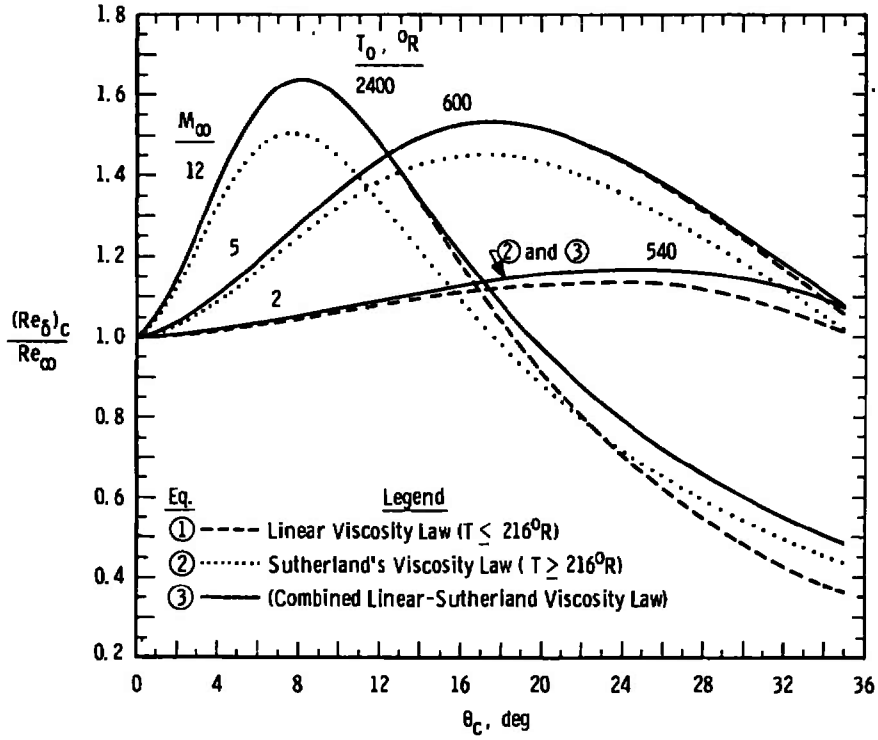

a. Sensitivity of the Reynolds Number Ratio to Viscosity Determinations

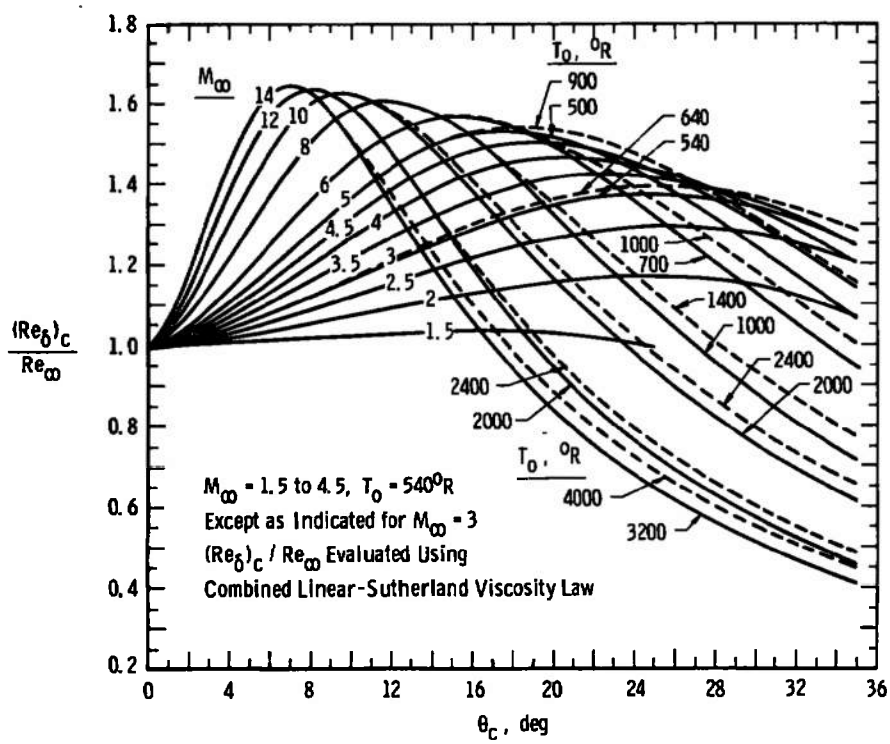

b. Variation of Reynolds Number Ratio with Cone Half-Angle, Mach Number and Temperature

Fig. 3 Inviscid Flow, Sharp Cone Reynolds Number Ratios for Air

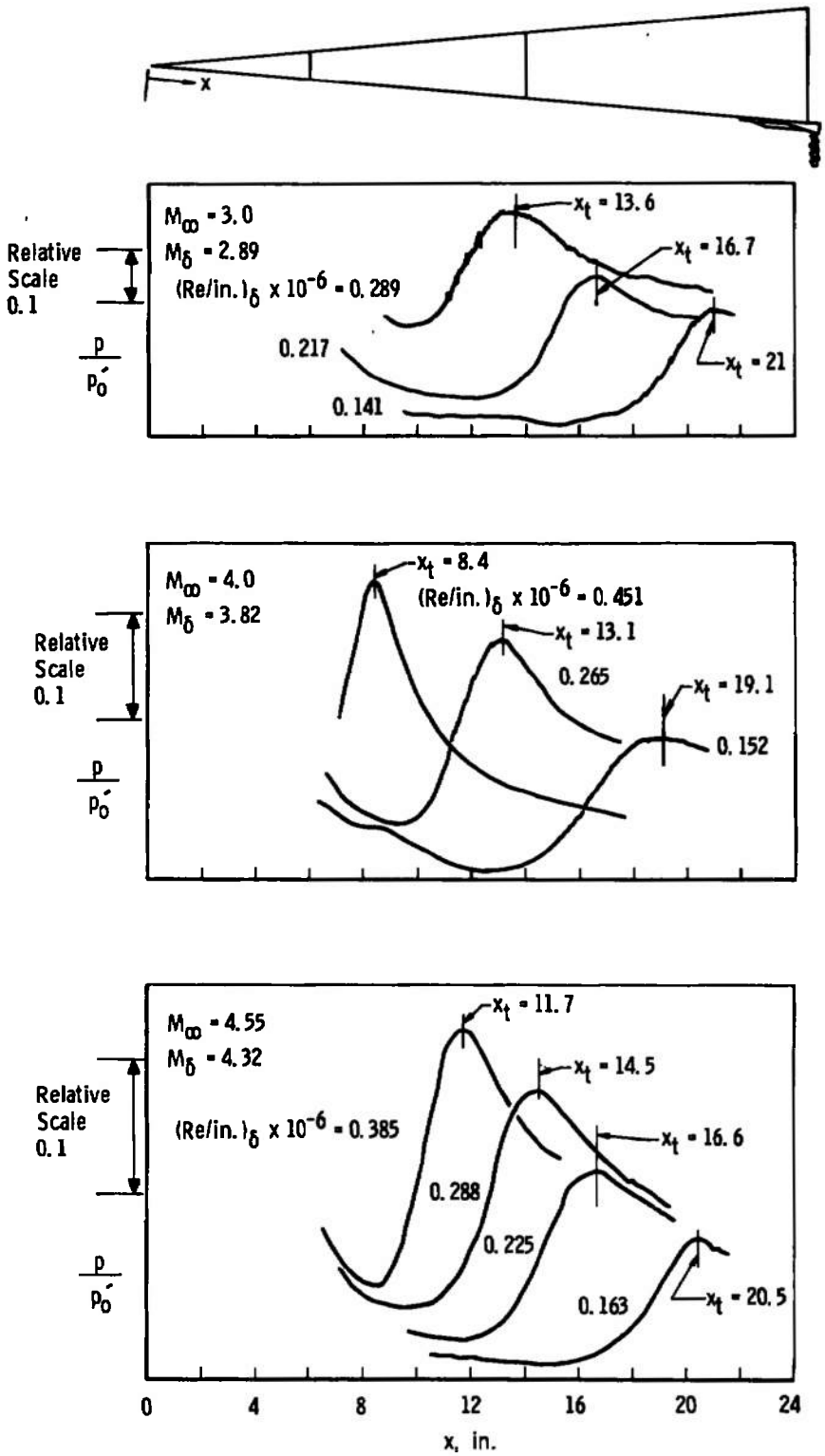

Fig. 4 Examples of Surface Probe Transition Profile Traces (Tunnel D)

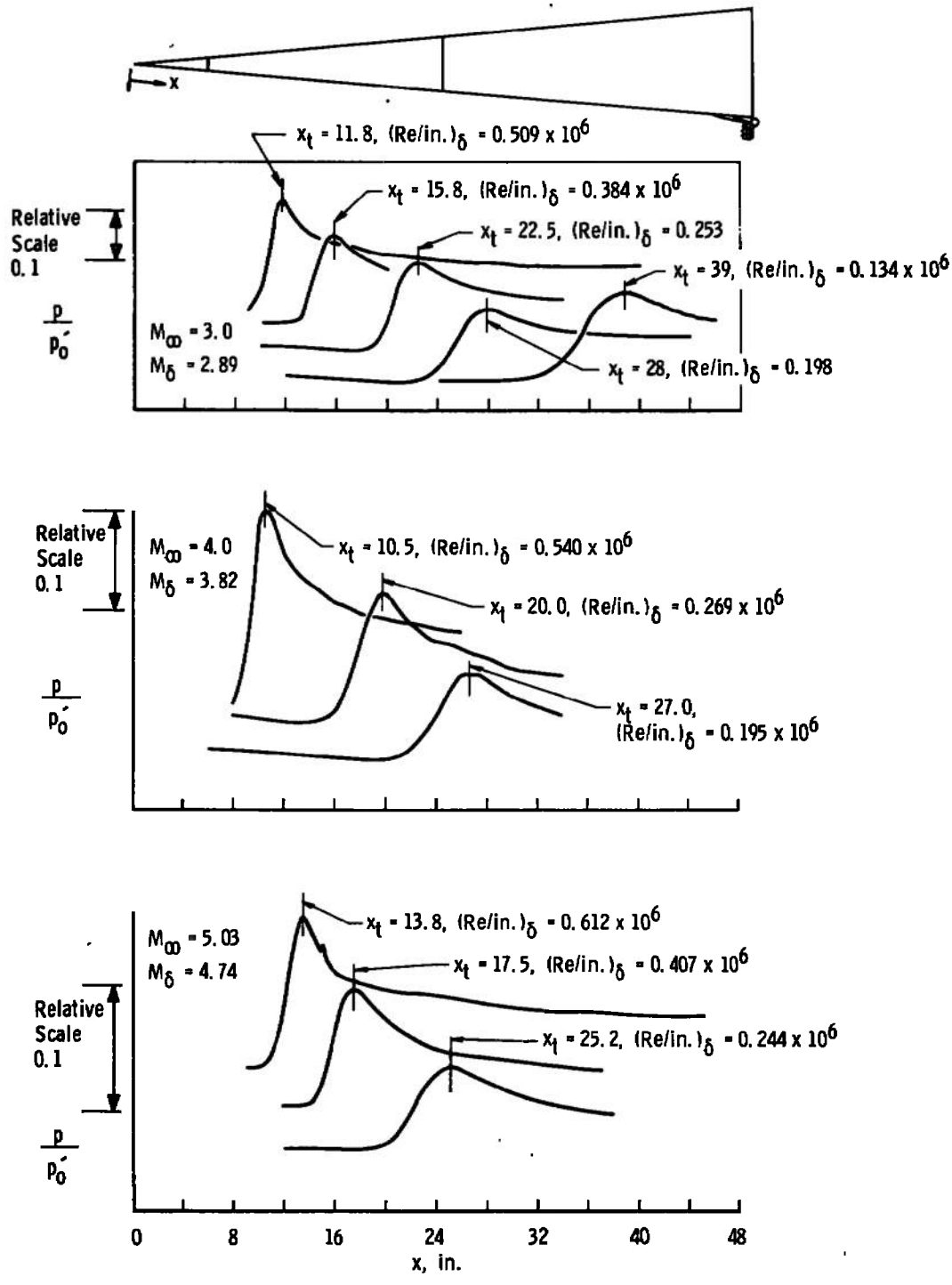

Fig. 5 Examples of Surface Probe Transition Profile Traces (Tunnel A)

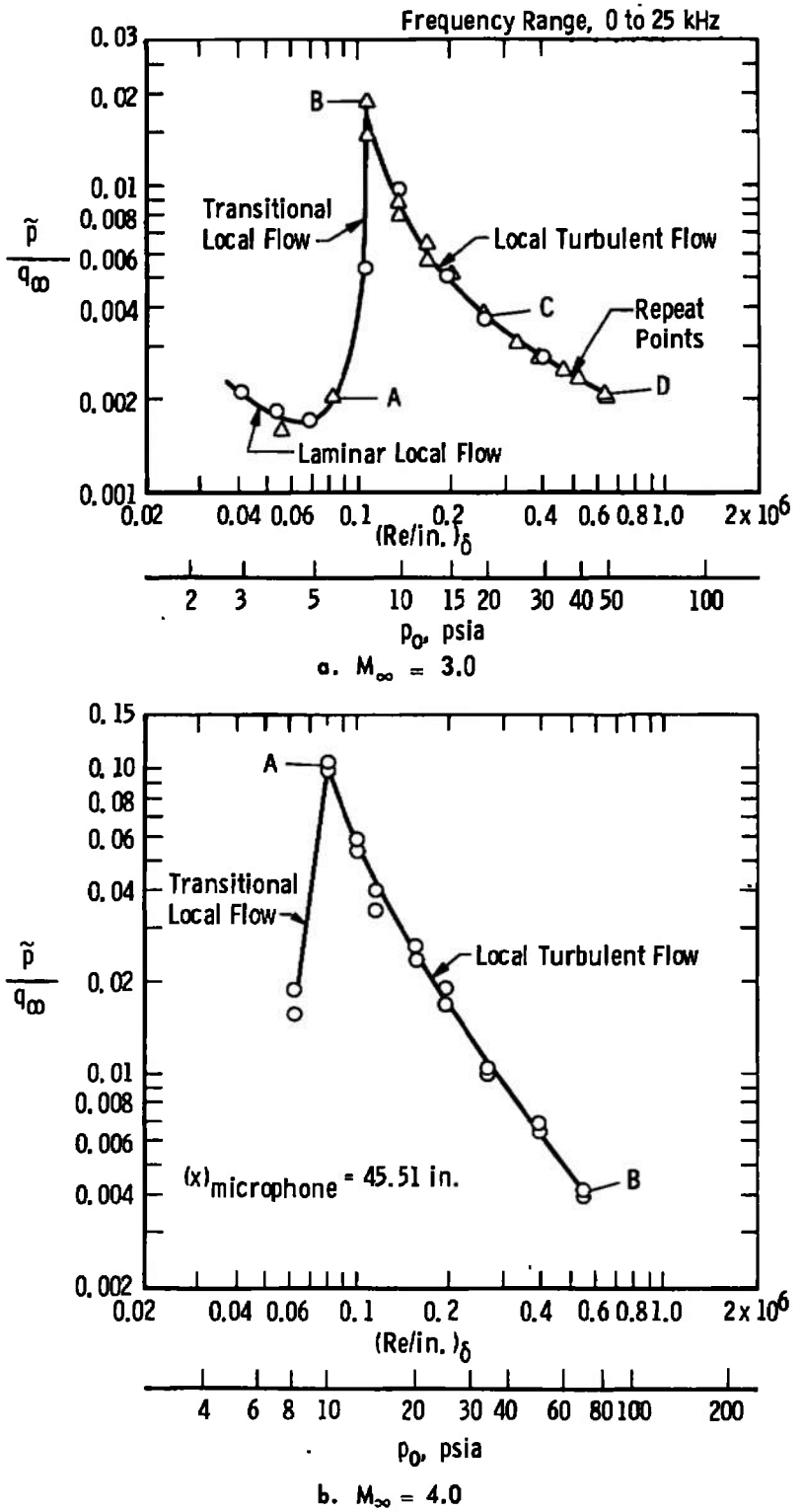

Fig. 6 Indication of Transition from Microphone Root-Mean-Square Pressure Fluctuations, M_∞ = 3 and 4

Sym	Configuration	Surface Ray	Method of Detection	Source	ℓ_m, in.
△	5-deg Cone	Top	Schlieren	Present Study	44
○	5-deg Cone	Bottom	Schlieren	Present Study	44
□	5-deg Cone	Bottom	Surface Probe (p_{max})	Present Study	44
—·—	Hollow Cylinder	Bottom	Surface Probe (p_{max})	Refs. 8, 9, and 13	48

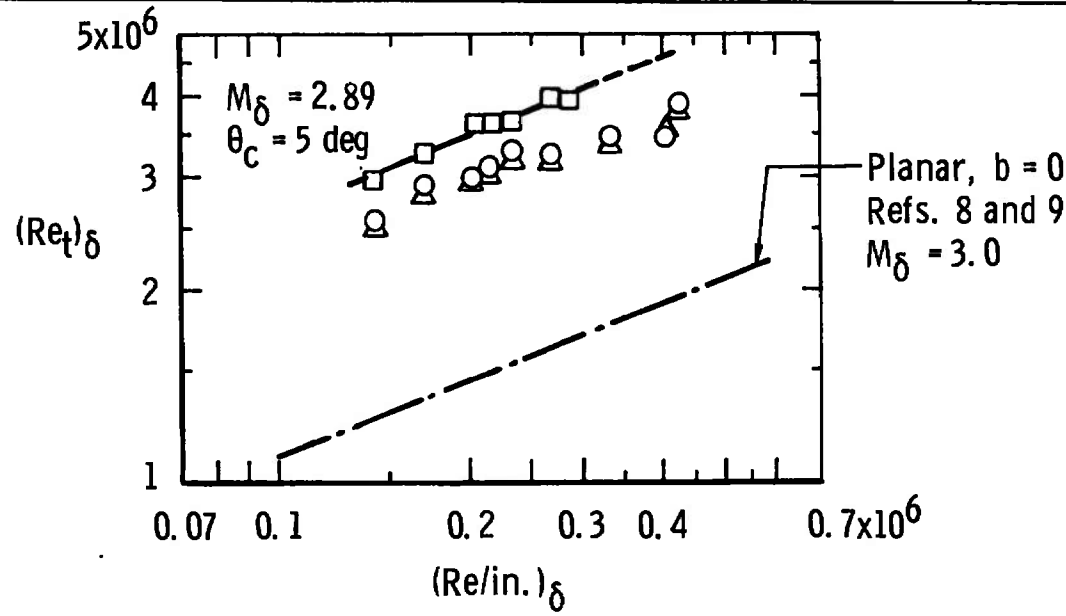

a. M_∞ = 3.0

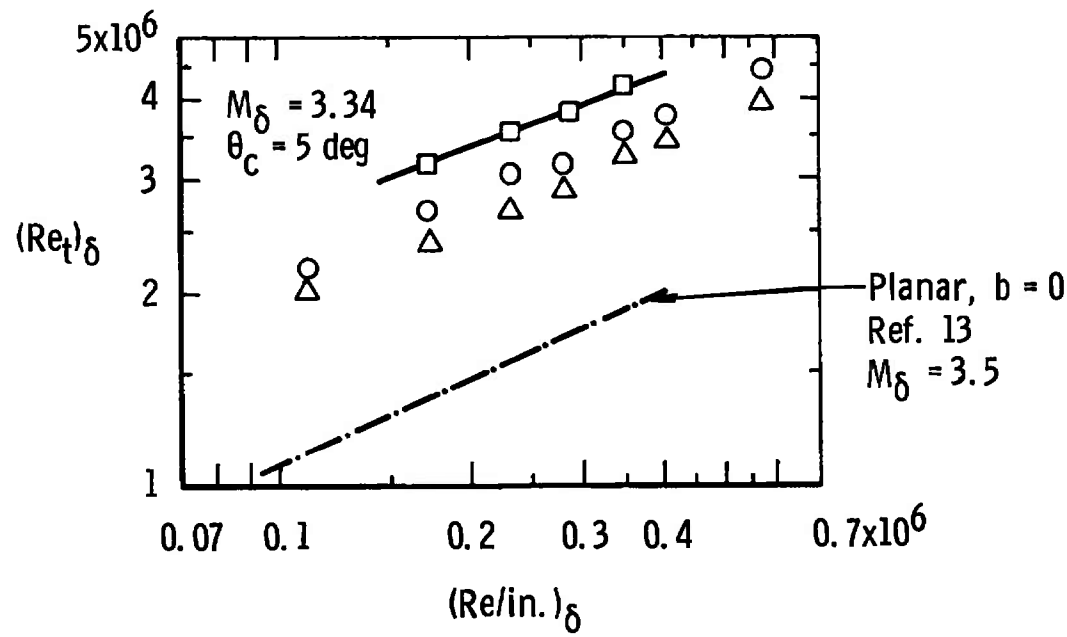

b. M_∞ = 3.48

Fig. 7 Transition Reynolds Number Data from Tunnel D, Sharp Cone and Planar Models

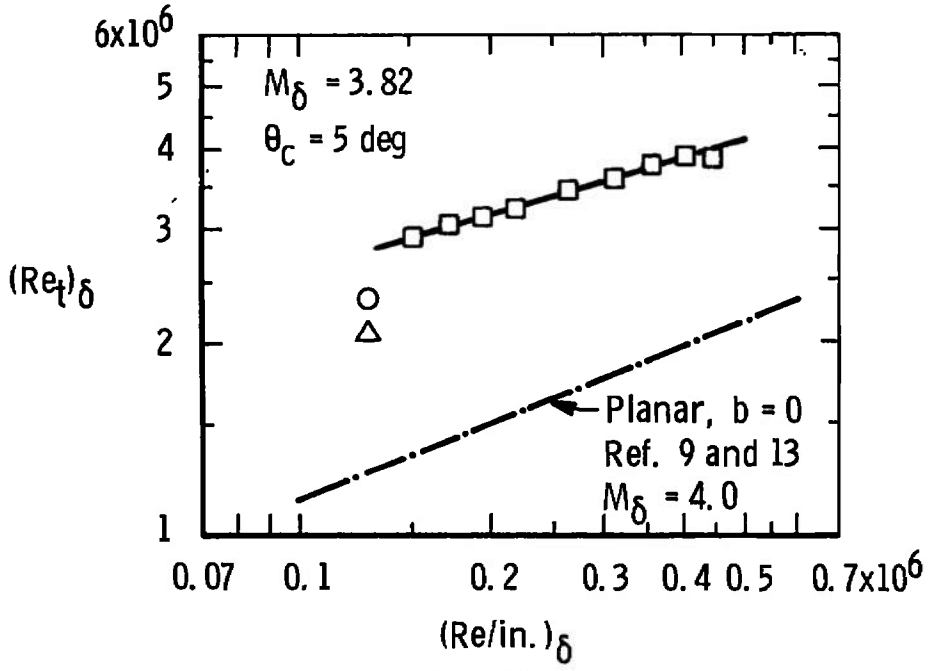

c. M_∞ = 4.0

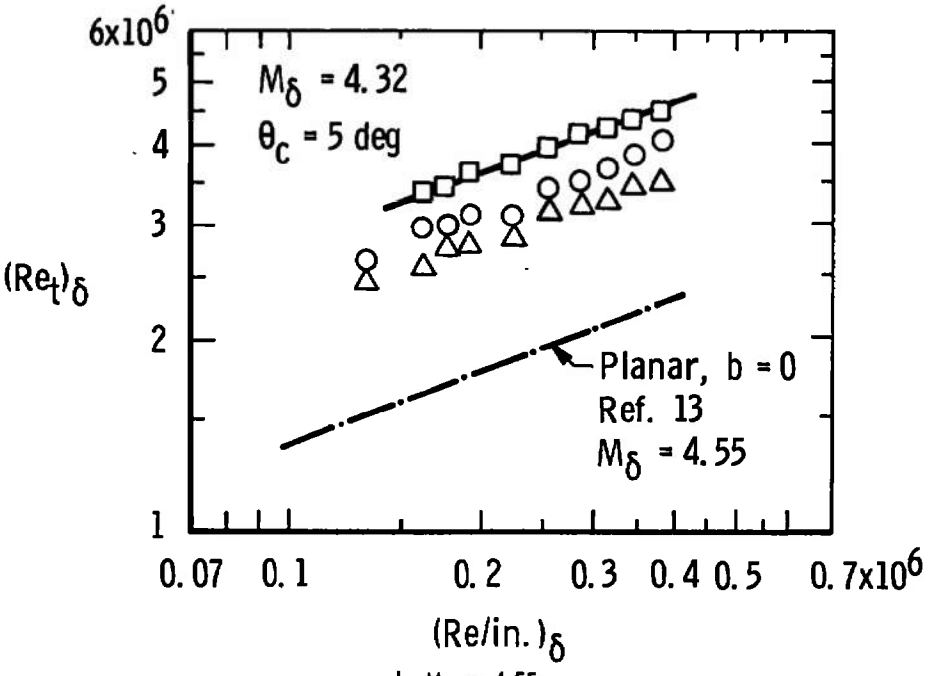

d. M_∞ = 4.55

Fig. 7 Concluded

Sym	Configuration	Surface Ray	Method of Detection	Source	ℓ_m, in.
△	5-deg Cone	Top	Shadowgraph	Present Study	215
○	5-deg Cone	Bottom	Shadowgraph	Present Study	215
□	5-deg Cone	Bottom	Surface Probe(p_{max})	Present Study	215
——	Hollow Cylinder	Side	Surface Probe(p_{max})	Refs. 8 and 9	213, 231
×	5-deg Cone	Top	Microphone($\tilde{p}_{max}$)	Present Study	215

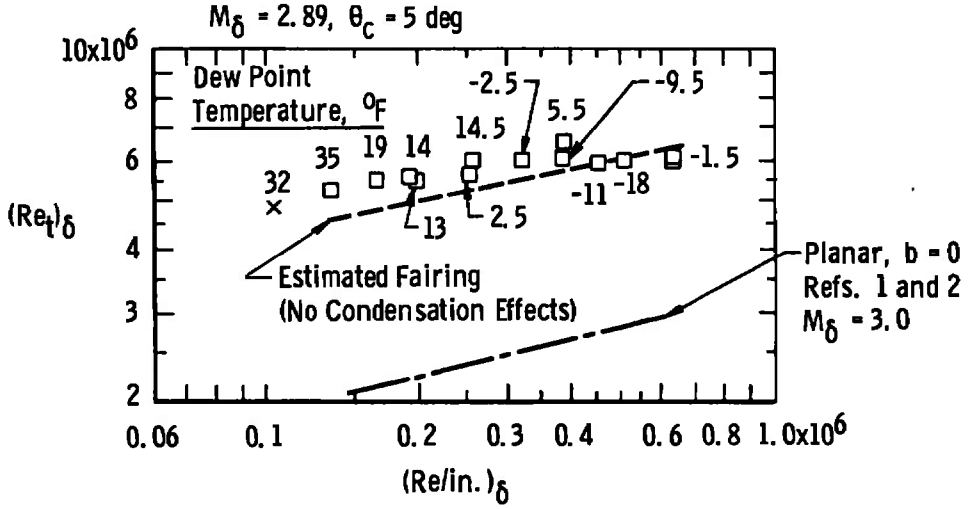

a. M_∞ = 3.0

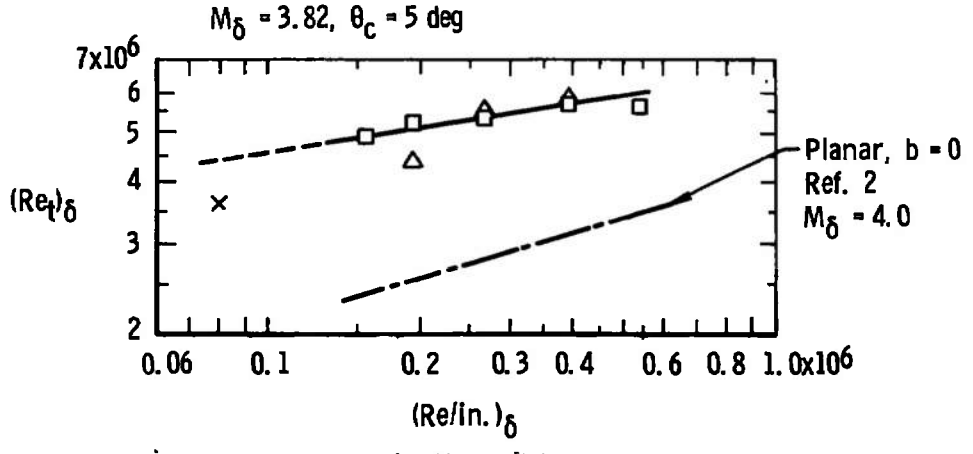

b. M_∞ = 4.0

Fig. 8 Transition Reynolds Number Data from Tunnel A, Sharp Cone and Planar Models

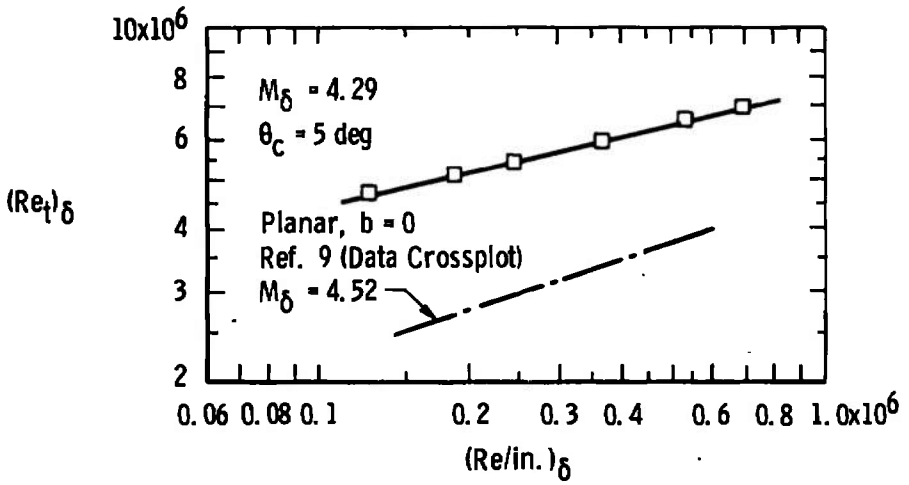

c. M_∞ = 4.52

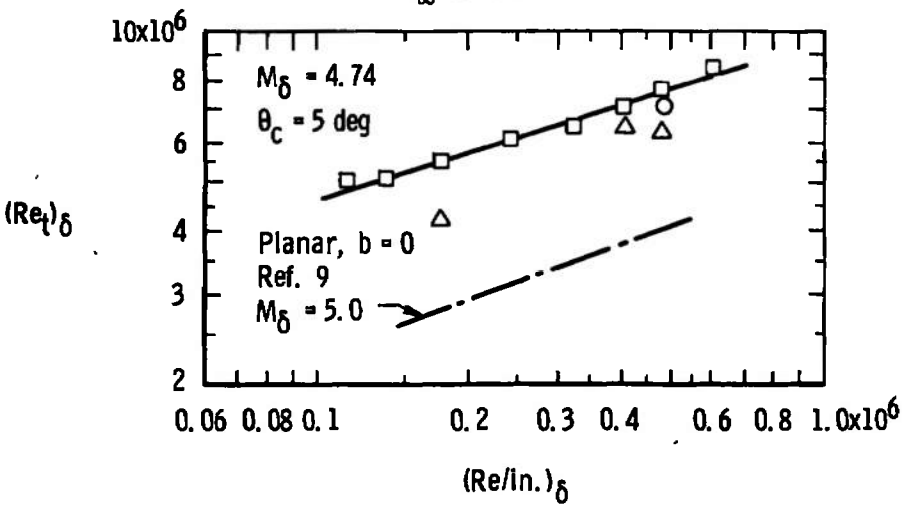

d. M_∞ = 5.03

M_δ = 5.5, θ_c = 5 deg, (T_0 = 719°R)

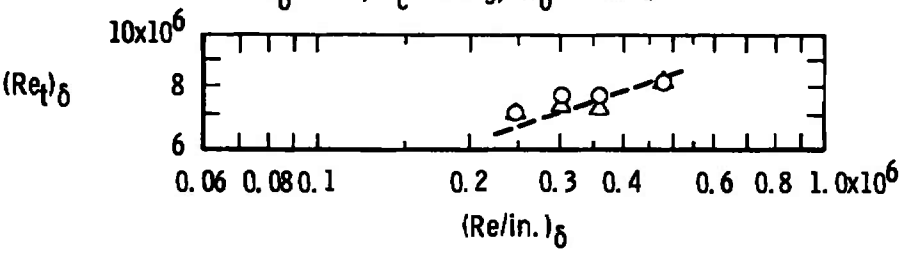

e. M_∞ = 5.94

Fig. 8 Concluded

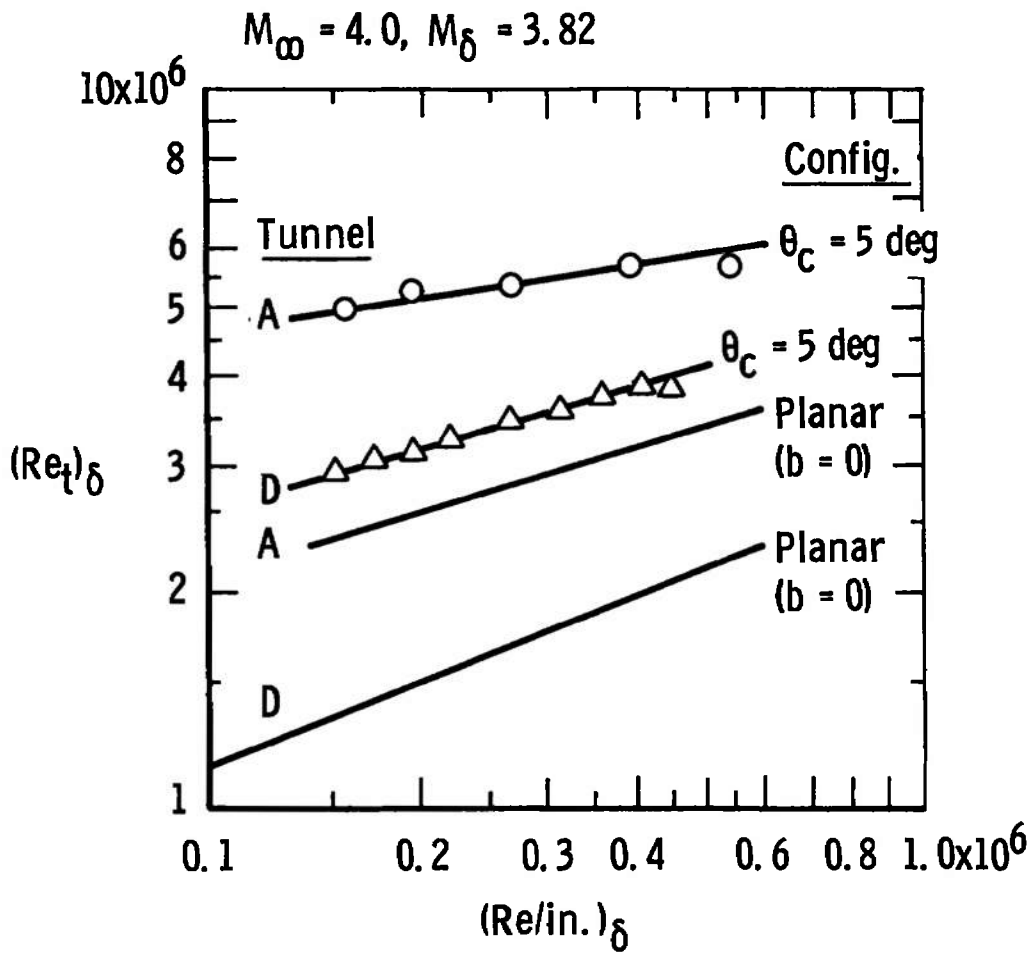

Fig. 9 Variation of Transition Reynolds Numbers with Tunnel Size

Planar Data and Eq. (4) from Refs. 8 and 9. Based on Data from Nine Different Wind Tunnel Facilities Varying in Size from 1 to 16 ft, Mach Number Range from 3 to 8, and $(Re/in.)_\infty$ Range from 0.05×10^6 to 1.1×10^6.

Symbol Notation for Cone Data Is Consistent with Table III.

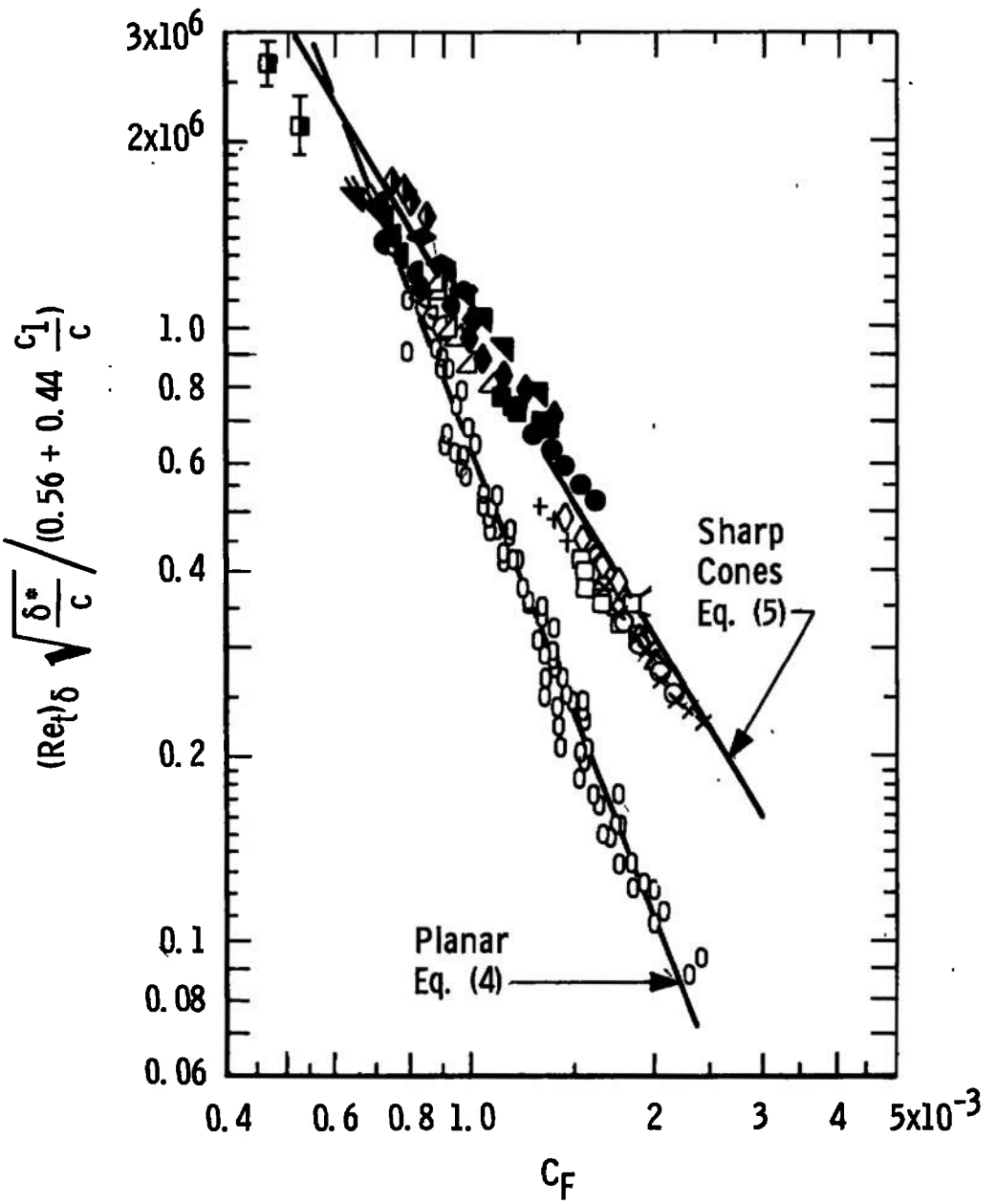

Fig. 10 Correlation of Transition Reynolds Numbers

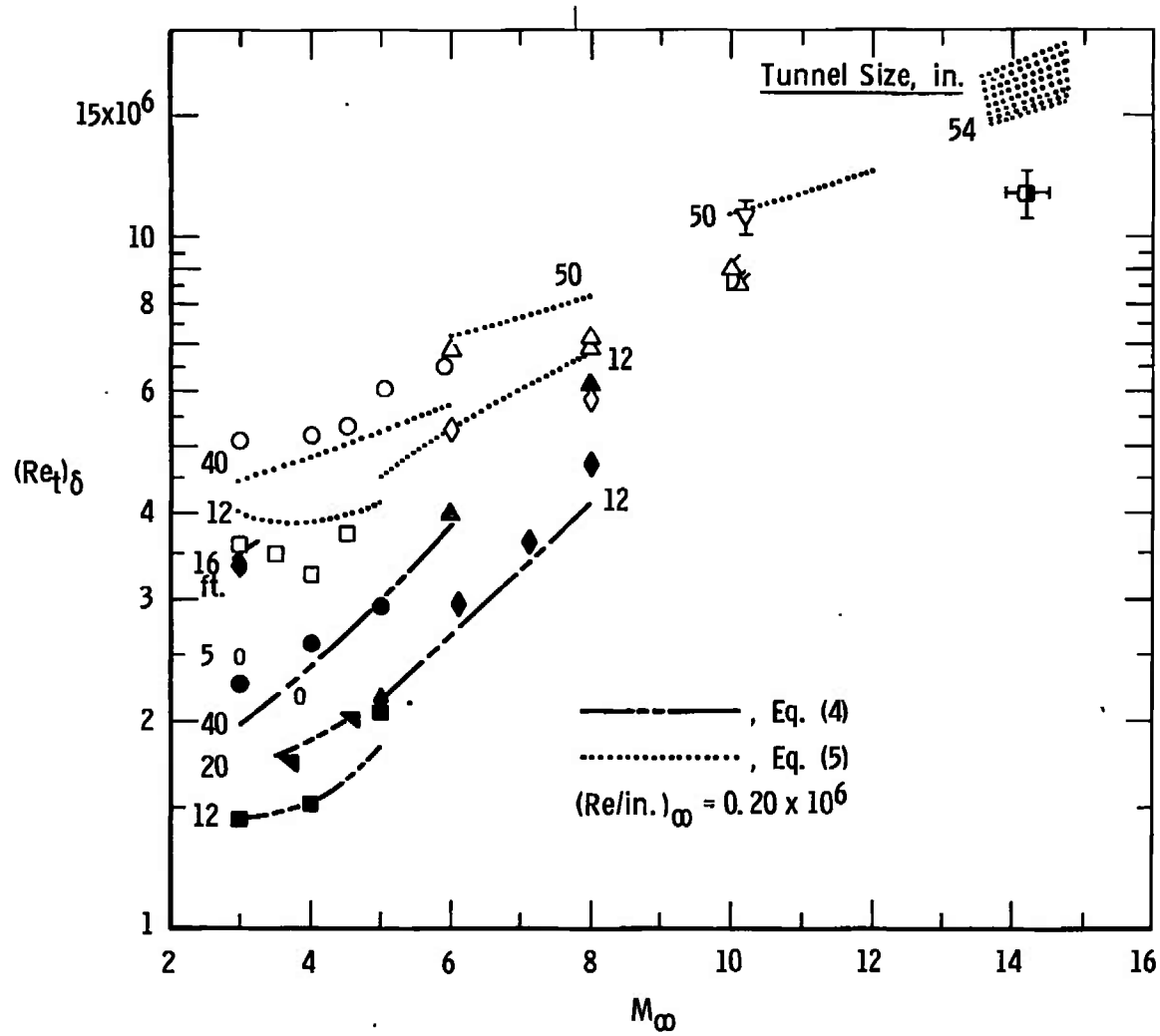

Fig. 11 Variation of Axisymmetric and Planar Transition Reynolds Numbers with Tunnel Size and Mach Number

Sym	M_∞	Configuration	Facility	Source	Method of Detection**
■	3, 4, 5	Hollow Cylinder, b = 0	AEDC VKF D(12 by 12 in.)	Refs. 8 and 9	Maximum P (No Adjustment)**
♦	5, 6.1, 7.1, 8	Flat Plate, b = 0	AEDC-VKF-E(12 by 12 in.)	Refs. 8 and 9	Maximum P (No Adjustment)**
◥	3.7, 4.6	Flat Plate, b = 0	JPL-SWT (18 by 20 in.)	Refs. 8 and 9	Maximum Surface Shear (No Adjustment)**
●	3, 4, 5	Hollow Cylinder, b = 0	AEDC-VKF-A (40 by 40 in.)	Refs. 8 and 9	Maximum P (No Adjustment)**
▲	6, 8	Hollow Cylinder and Flat Plate, b = 0	AEDC-VKF-B (50-in. Diam)	Refs. 8 and 9	Maximum P (No Adjustment)**
* ◆	3	Hollow Cylinder	AEDC-PWT-16S (16 by 16 ft)	Refs. 8 and 9	Maximum P (No Adjustment)**
□	3, 3.5, 4, 4.5	Sharp Cone, θ_c = 5 deg	AEDC VKF-D (12 by 12 in.)	Present Study	Maximum P (No Adjustment)**
○	3, 4, 4.5, 5, 5.9	Sharp Cone, θ_c = 5 deg	AEDC-VKF-A (40 by 40 in.)	Present Study	Maximum P (M_∞ = 5.9, Shadowgraph) (No Adjustment)**
* ◇	6.1, 8	Sharp Cone, θ_c = 10 deg	AEDC-VKF-E (12 by 12 in.)	Ref. 10	Shadowgraph (Adjusted by Factor of 1.1)
0	3.1, 3.8	Sharp Cone, θ_c = 7.5 deg	R.A.E. (5 by 5 in.)	Ref. 36	Shadowgraph (No Adjustment)
V	10.2	Sharp Cone, θ_c = 3.75 deg	NASA Langley (31 by 31 in.)	Ref. 34	Maximum $\dot{q}$ ($0.4 < (T_w/T_0) \leq 0.63$) (No Adjustment)
D	10	Sharp Cone, θ_c = 5 deg	Republic Aviation Corp. (36-in. Diam)	Ref. 37	Maximum $\dot{q}$ ($0.075 \leq (T_w/T_0) \leq 0.36$)(No Adjustment)
⩘	10	Sharp Cone, θ_c = 6 deg	AEDC-VKF-C (50-in. Diam)	Ref. 33	Maximum $\dot{q}$ ($(T_w/T_0) = 0.25$) (No Adjustment)
△	8	Sharp Cone, θ_c = 9 deg	AEDC-VKF-B (50-in. Diam)	VKF and Ref. 10	Shadowgraph ($(T_w/T_0) \approx 0.8$, Hot Wall) (No Adjustment)
△	6	Sharp Cone, θ_c = 6 deg	AEDC-VKF-B (50-in. Diam)	VKF and Ref. 10	Maximum $\dot{q}$ ($(T_w/T_0) \approx 0.63$)(Adjusted by Factor of 1.08)
⩘	10	Sharp Cone, θ_c = 9 deg	AEDC-VKF-C (50-in. Diam)	VKF	Shadowgraph ($(T_w/T_0) \approx 0.66$, Hot Wall)(Adjusted by Factor of 1.1)
◨	14.2 ± 0.3	Sharp Cone, θ_c = 9 deg	AEDC-VKF-F (54-in. Diam)	Ref. 11	Maximum $\dot{q}$ ($(T_w/T_0) \approx 0.19$)(No Adjustment)

*Extrapolated Data

**Amount of Adjustment Based on Results of Present Study and Refs. 10, 13, and 14

Fig. 11 Concluded

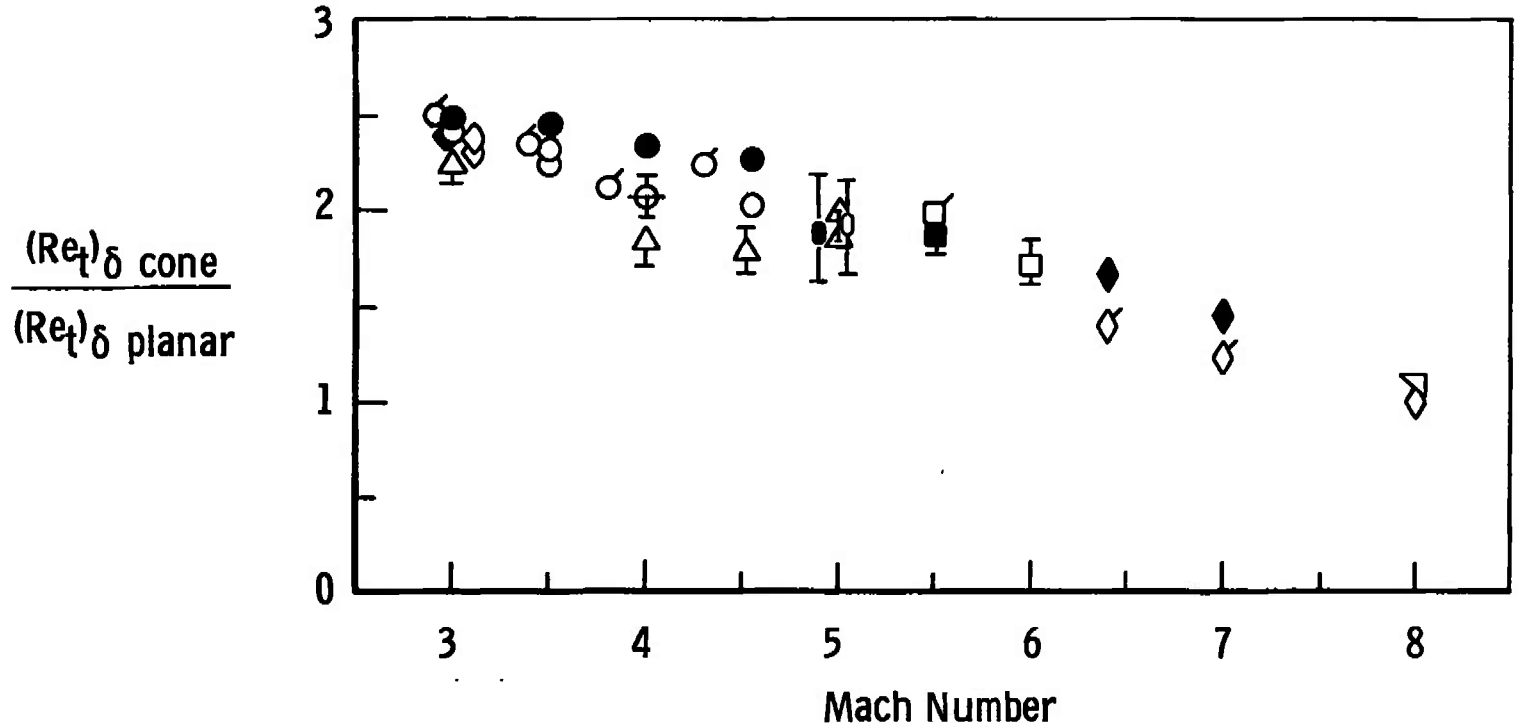

Fig. 12 Correlation of Axisymmetric and Planar Transition Reynolds Number Ratios

Sym	Configuration	θ_c, deg	M_∞	M_δ	$(Re/in.)_\delta \times 10^{-6}$ Range	Facility	Method-of-Detection	Source
○	Sharp Cone	5	3 to 4.5	2.9 to 4.3	0.15 to 0.4	VKF-D (12 by 12 in.)	Maximum Pitot Pressure	Present Study (Fig. 7)
	Hollow Cylinder (b = 0)	-	3 to 4.5	3 to 4.5				Refs. 8, 9, and 13
△	Sharp Cone	5	3 to 5	2.9 to 4.7	0.15 to 0.6	VKF-A (40 by 40 in.)	Maximum Pitot Pressure	Present Study (Fig. 8)
	Hollow Cylinder (b = 0)	-	3 to 5	3 to 5				Ref. 9
□	Sharp Cone	5, 6	6	5.5	0.15 to 0.4	VKF-A and VKF-B (50-in. Diam)	Shadowgraph $\dot{q}_{maximum}$	Present Study VKF
	Flat Plate (b ≈ 0)	-	6	6				Refs. 9 and 38
◇	Sharp Cone	6, 9	8	7.0, 6.4	0.2, 0.3	VKF-B (50-in. Diam)	$\dot{q}_{max}$ and Shadowgraph	Refs. 10 and VKF
	Hollow Cylinder (b = 0)	-	8	8			$(T_w)_{max}$ and Pitot Pressure	Ref. 14
◁	Sharp Cone	6, 9	8	7.0, 6.4	0.2	VKF-B (50-in. Diam)	$\dot{q}_{max}$ and Shadowgraph	Ref. 10 and VKF
	Flat Plate (b ≈ 0)	-	8	8			Pitot Pressure	Ref. 39
◇	Sharp Cone	5	3.1	2.98	0.1 to 0.6	NACA-Lewis (12 by 12 in.)	$T_{w\,max}$	Ref. 15
	Hollow Cylinder	-	3.1	3.1				
o	Sharp Cone	2.5	5.0	4.90	0.15 to 0.5	NASA-Lewis (12 by 12 in.)	$T_{w\,max}$	Ref. 16
	Hollow Cylinder	-	5.0	5.0				

Flagged Symbols - Evaluated at Equivalent $(Re/in.)_\delta$ and M_δ Values $[(Re/in.)_\delta = 0.2 \times 10^6$

Open Symbols - Evaluated at Equivalent $(Re/in.)_\delta$ and M_∞ Values

Solid Symbols - Evaluated at Equivalent $(Re/in.)_\infty$ and M_δ Values (From Data Cross Plots)

Fig. 12 Concluded

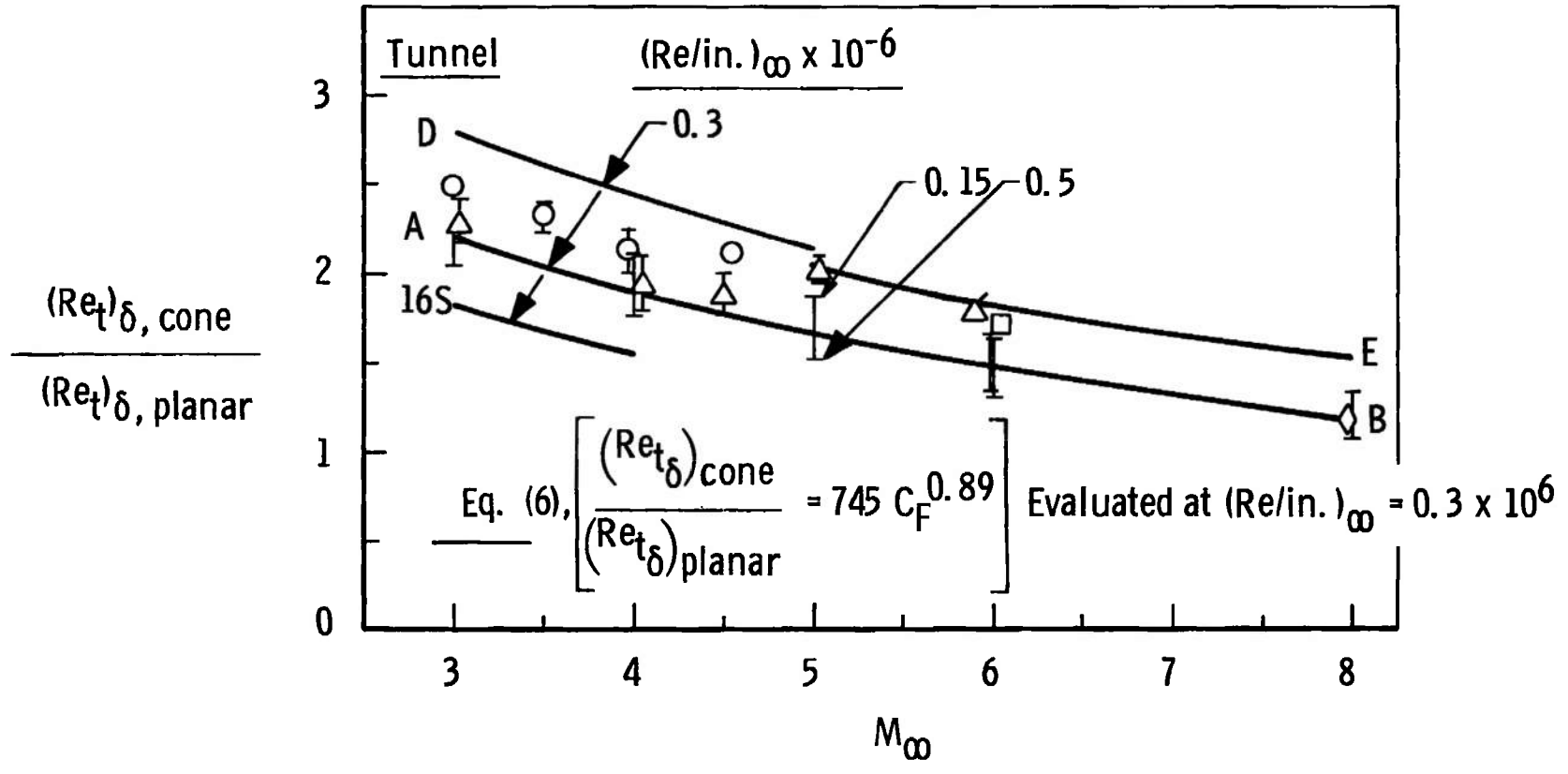

Fig. 13 Comparison of Predicted and Measured Cone-Planar Transition Ratios

Experimental Data Evaluated at Equivalent $(Re/in.)_\infty$ and M_∞ Values

Sym	Configuration	θ_c, deg	M_∞	M_δ	$(Re/in.)_\infty \times 10^{-6}$ Range	Facility	Method of x_t Detection	Source
○	Sharp Cone	5	3 to 4.5	2.9 to 4.3	0.15 to 0.5	VKF-D (12 by 12 in.)	Maximum Surface Pitot Probe Pressure	Present Study
	Hollow Cylinder (b = 0)	-	3 to 4.5	3 to 4.5	0.15 to 0.5			Refs. 9 and 13
△	Sharp Cone	5	3 to 5	2.9 to 4.7	0.15 to 0.5	VKF-A (40 by 40 in.)	Maximum Surface Pitot Probe Pressure	Present Study
	Hollow Cylinder (b = 0)	-	3 to 5	3 to 5	0.15 to 0.5			Ref. 9
◁	Sharp Cone	5	5.9	5.5	0.2	VKF-A (40 by 40 in.)	Schlieren	Present Study
	Hollow Cylinder (b = 0)	-	5.9	5.9	0.2		Schlieren	Data Extrapolation from Refs. 8 and 9
□	Sharp Cone	6	6	5.5	0.2	VKF-B (50-in. Diam)	Adjusted Max Heat Transfer (Adjusted by 1.08)	Ref. 10 and VKF
	Flat Plate (b = 0)	-	6	6	0.2		Maximum Pitot Press.	Refs. 9 and 38
◇	Sharp Cone	6, 9	8	7.0, 6.4	0.15 to 0.3	VKF-B (50-in. Diam)	Maximum Heat Trans. (No Adjustment)	Ref. 10 and VKF
	Hollow Cylinder (b = 0)	-	8	8	0.15 to 0.3		Maximum Pitot Press.	Ref. 14

Fig. 13 Concluded

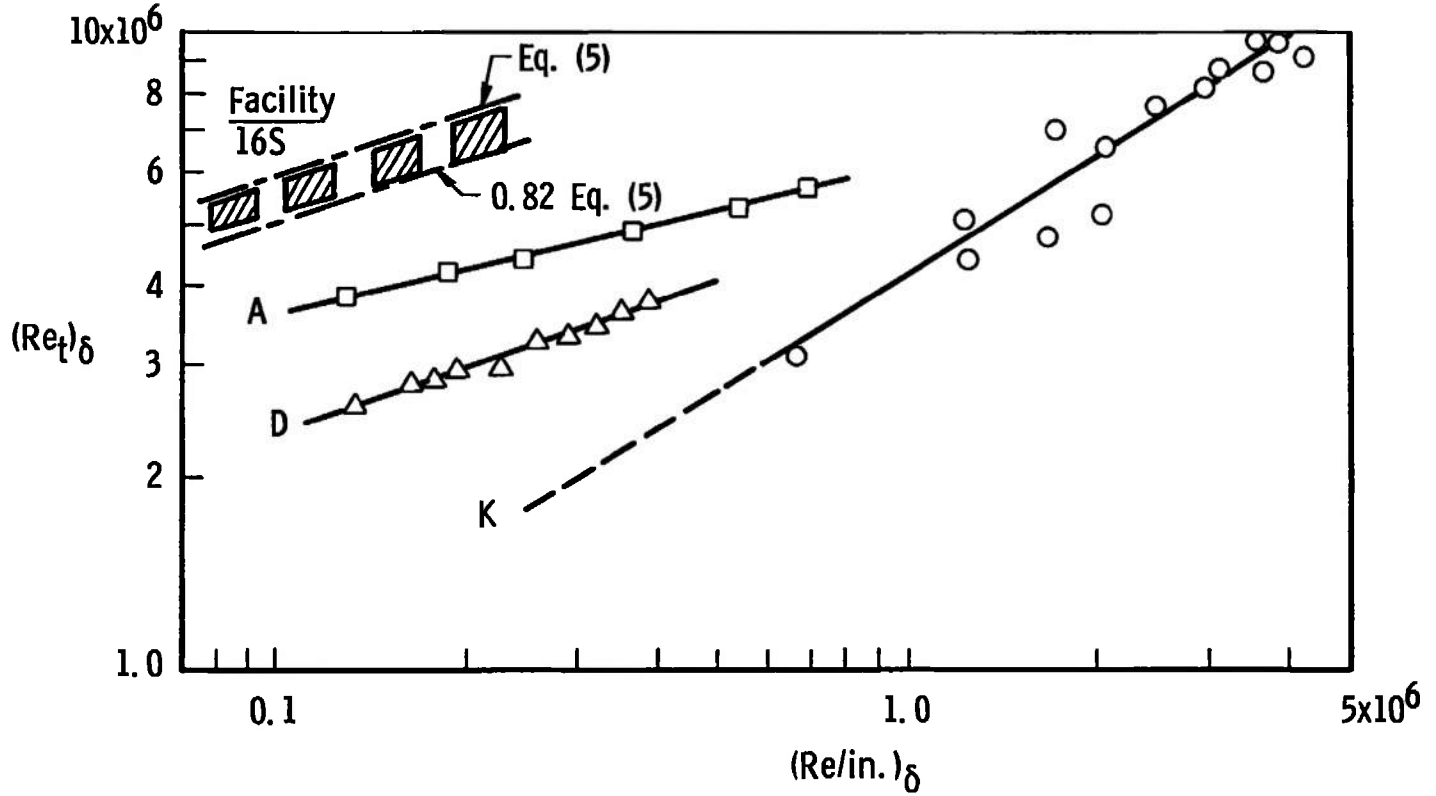

Fig. 14 Comparison of Sharp Cone Transition Reynolds Numbers from Wind Tunnels and an Aeroballistic Range

Sym	Facility	M_δ	T_w/T_{aw}	θ_c, deg	Source	Method of Detection
○	VKF Range K	4.3	≈ 0.18	10	Ref. 24	Shadowgraph - Schlieren
△	VKF Tunnel D (12 by 12 in.)	4.3	≈ 1.0	5	Present Study	Schlieren
□	VKF Tunnel A (40 by 40 in.)	4.3	≈ 1.0	5	Present Study	Surface Pitot Probe Maximum Value Adjusted to Schlieren Location $(Re_t)_{schlieren} \approx 0.82\,(Re_t)_{p_{max}}$
▨	PWT-Tunnel 16S (16 by 16 ft)	4.3	≈ 1.0	5	Present Study and Refs. 8 and 9	Estimated from Two-Dimensional Data Surface Probe Data

Fig. 14 Concluded

TABLE I
TUNNEL D TRANSITION REYNOLDS NUMBER, 10-DEG TOTAL-ANGLE SHARP CONE

M_∞	$M_C = M_\delta$	p_O, psia	T_O, °R	$(Re/in.)_\infty \times 10^{-6}$	$(Re/in.)_\delta \times 10^{-6}$	x_t,* in.	$(Re_t)_\delta \times 10^{-6}$
2.98	2.87	9.93	533	0.133	0.141	≈21	≈2.97
2.99	2.88	14.9	524	0.204	0.217	16.7	3.62
3.00	2.89	20.0	523	0.272	0.289	13.6	3.93
2.98	2.87	9.86	532	0.133	0.141	≈21	≈2.96
2.99	2.88	12.4	544	0.160	0.170	19.3	3.28
2.99	2.88	14.9	548	0.191	0.203	17.8	3.61
3.00	2.89	17.4	549	0.220	0.234	15.7	3.67
3.00	2.89	20.0	549	0.253	0.269	14.8	3.98
3.48	3.34	15.0	520	0.160	0.172	18.5	3.18
3.48	3.34	20.0	516	0.215	0.232	15.3	3.54
3.48	3.34	24.8	514	0.269	0.289	13.2	3.82
3.48	3.34	30.0	513	0.326	0.350	12.0	4.20
3.99	3.81	17.5	530	0.139	0.152	19.1	2.91
4.00	3.82	20.0	528	0.159	0.174	17.6	3.07
4.00	3.82	22.5	526	0.180	0.197	15.8	3.12
4.00	3.82	24.9	523	0.201	0.220	14.7	3.24
4.00	3.82	29.9	521	0.242	0.265	13.1	3.47
4.00	3.82	34.9	518	0.286	0.313	11.5	3.60
3.99	3.81	39.9	518	0.328	0.359	10.5	3.77
3.99	3.81	45.0	517	0.371	0.407	9.4	3.83
3.99	3.81	50.0	518	0.411	0.451	8.4	3.78
4.55	4.32	24.9	539	0.146	0.163	≈20.5	3.34
4.56	4.33	27.4	540	0.159	0.177	19.5	3.46
4.56	4.33	29.9	542	0.173	0.193	18.9	3.65
4.56	4.33	34.9	543	0.202	0.225	16.6	3.74
4.56	4.33	39.9	544	0.229	0.255	15.6	3.98
4.56	4.33	45.0	546	0.258	0.288	14.5	4.17
4.56	4.33	49.9	547	0.285	0.318	13.5	4.29
4.56	4.33	55.0	548	0.312	0.348	12.6	4.38
4.55	4.32	60.0	546	0.345	0.385	11.7	4.50

*x_t Determined from Surface Probe Peak Pressure

TABLE II
TUNNEL A TRANSITION REYNOLDS NUMBERS, 10-DEG TOTAL-ANGLE SHARP CONE

M_∞	$M_c = M_\delta$	p_o, psia	T_o, °R	$(Re/in.)_\infty \times 10^{-6}$	$(Re/in.)_\delta \times 10^{-6}$	x_t,* in.	$(Re_t)_\delta \times 10^{-6}$	Dew Point Temperature, °F
2.99	2.88	19.8	562	0.243	0.258	23.3	6.01	14.5
2.99	2.88	29.7	562	0.364	0.387	17.0	6.57	5.5
2.99	2.88	14.8	565	0.181	0.192	29.0	5.57	14.0
2.98	2.88	10.1	561	0.126	0.134	39.2	5.25	35
3.00	2.89	49.9	566	0.603	0.640	9.5	6.08	- 1.5
3.00	2.89	49.6	569	0.596	0.633	9.3	5.89	- 1
3.00	2.89	39.8	568	0.479	0.509	11.8	6.00	-18
3.00	2.89	35.0	566	0.424	0.450	13.3	5.99	-11
2.99	2.88	29.6	565	0.362	0.384	15.8	6.07	- 9.5
2.99	2.88	24.7	563	0.303	0.322	18.7	6.02	- 2.5
2.99	2.88	19.7	568	0.238	0.253	22.5	5.69	2.5
2.99	2.88	15.1	562	0.186	0.198	28.0	5.53	13
2.98	2.87	12.6	561	0.156	0.166	33.2	5.51	19
4.02	3.84	69.9	569	0.493	0.540	10.5	5.67	-10.5
4.02	3.84	50.0	562	0.359	0.394	14.6	5.75	-10
4.02	3.84	34.6	565	0.246	0.269	20.0	5.38	- 4.5
4.01	3.83	24.7	563	0.178	0.195	27.0	5.25	8.0
4.00	3.82	19.8	564	0.143	0.157	31.6	4.95	12
4.54	4.31	116	573	0.623	0.695	10.0	6.95	-19.5
4.53	4.30	89.6	573	0.483	0.539	12.2	6.57	-23
4.53	4.30	59.7	568	0.327	0.365	16.4	5.98	-19
4.53	4.30	39.6	565	0.218	0.243	22.3	5.42	-12
4.52	4.29	29.8	564	0.166	0.185	≈28	≈5.2	- 3.5
4.50	4.27	19.7	563	0.111	0.124	≈38	≈4.7	8.0
5.04	4.75	150	646	0.532	0.612	13.8	8.44	-18
5.06	4.77	120	644	0.420	0.483	15.8	7.63	-14
5.05	4.76	101	645	0.354	0.407	17.5	7.12	-17
5.05	4.76	79.9	646	0.281	0.323	20.2	6.53	-13.5
5.04	4.75	59.9	645	0.212	0.244	25.2	6.14	-12
5.02	4.73	40.2	616	0.154	0.177	31.2	5.53	- 2.5
5.00	4.71	29.9	600	0.120	0.138	37.0	5.11	6.5
5.00	4.71	24.9	602	0.100	0.115	≈44	5.06	14.5

*x_t Determined from Surface Probe Peak Pressure

TABLE III
SOURCE AND RANGE OF DATA USED IN THE TRANSITION REYNOLDS NUMBER CORRELATION (FIG. 10)

Source	Symbol	M_∞	M_δ	$h \times 10^3$	θ_c, deg	$(Re/in)_\infty \times 10^{-6}$	Tunnel	Test Section Size	Method of Transition Detection	*Amount of Adjustment	t_{m}, in	T_w/T_{aw}	T_w/T_0	Method of δ^* Determination	
Present Study	○	3	2.9	5 (Sharp)	5	0.15 to 0.4	AEDC - VKF D	12 by 12 in	Maximum Probe Pressure	No Adjustment	44	≈1.0	0.80	Experimental Data	t_T = 56 in.
	△	3.5	3.4												Ref 29
	□	4	3.8												
	◇	4.55	4.3												
Present Study	●	3	2.9	5 (Sharp)	5	0.15 to 0.6	AEDC - VKF A	40 by 40 in	Maximum Probe Pressure	No Adjustment	216	≈1.0	≈0.90	Experimental Data	t_T = 200 to
	■	4	3.8												Refs 9 and 28
	◆	4.5	4.1												
	◀	5	4.7												
	◆	5.9	5.5						Shadowgraph						
Ref 10 and VKF	◆ **	8	5.5	Sharp	8	0.16 to 0.43	AEDC - VKF B	50-in Diam	Maximum q	1.08	245	0.72	0.63	VKF Experimental	
	◖ **	8	7.0		6	0.16 to 0.29			Maximum q	No Adjustment		0.48	0.41	Data and Ref 30	
	◖	8	8.4		0	0.12 to 0.29			Shadowgraph	No Adjustment		≈0.03	≈0.81	t_T = 244 in	
Ref 33	⋎ ▲▲	10	8.5	Sharp	6	0.13	AEDC - VKF C	50-in Diam	Maximum q	No Adjustment	>300	≈0.29	≈0.25	VKF Experimental	
Ref 10	⋎	18	7.5	Sharp	9	0.17	AEDC - VKF C	50-in Diam	Shadowgraph	1.1	>300	≈0.77	≈0.60	Data, t_T > 300 in	
Ref 11	⊓ ▲▲ ‡	14.2	9.7	4 (Sharp)	9	0.12, 0.2	AEDC - VKF F (Hotshot)	54-in Diam	Maximum q	No Adjustment	350	≈0.22	≈0.19	Ref 32, t_T = 304 in	
Ref 10	◁ --	6	5.0	Sharp	10	0.34 to 1.2	AEDC - VKF E	12 by 12 in	Shadowgraph	1.1	≈64	≈0.86	≈0.75	Estimated	t_T = 64 in
	◁	8	8.2			0.35 to 0.54				1.1		≈0.8	≈0.5	Using δ^+	
Ref 34	◆ **	10.2	5.2	4 to 10 (Sharp)	3.75	0.10 to 0.19	NASA Langley	31 by 31-in Hypersonic	Maximum q	No Adjustment	158	0.43 to 0.63	0.37 to 0.54	Correlation Refs 8 or 9	t_T = 158 in.
Ref 15	×	3.1	3.0	3 (Sharp)	5	0.1 to 0.67	NACA - Lewis	12 by 12 in	Maximum T_w	1.18	≈40	≈1.0	≈0.00		t_T = 47 in
Ref 16	+	5.0	4.9	3 (Sharp)	2.5	0.16 to 0.47	NASA - Lewis	12 by 12 in	Maximum T_w	1.13	≈47	≈1.0	≈0.00		t_T = 55 to
Ref. 35	□	9.84	9.87	1 (Sharp)	5	0.18 to 0.48	IPI - SWT	0 by 12 in	Maximum T_w	1.19	≈49	≈1.0	≈0.80	Experimental Data Ref. 31, t_T = 48 to	

*Adjustment for Method of Detection Based on Refs 13 and 14

**Cool-Wall Model

‡Nitrogen Test Gas

TABLE IV
ESTIMATED CONE-PLANAR TRANSITION RATIOS

1	2		3	4	5	6	7
Tunnel	Free-Stream Conditions		Experimental (Fig. 11)	Theoretical (Ref. 22)	Critical Reynolds Number from Stability Experiments Ref. 12	$1 + 2\left(\frac{\delta}{\delta}\right)$ Estimated, Eq. (7)	$1 + 2\left(\frac{\delta}{\delta/2}\right)$ Estimated, Eq. (7) with Adjustments
	M_∞	$(Re/in.)_\infty \times 10^{-6}$	$(Re_t)_{\delta,\,planar} \times 10^{-6}$	$(Re_t)_{\delta}$ planar-minimum $\times 10^{-6}$		$\frac{(Re_t)_{\delta,\,cone}}{(Re_t)_{\delta,\,planar}}$	
D	3	0.2	1.42	0.016	≈0.08	1.022	1.23
A	3		2.25	0.016	≈0.08	1.014	1.14
16S	3		3.35	0.016	≈0.08	1.010	1.10
D	5		2.05	0.044	≈0.5	1.042	1.98
A	5		2.95	0.044	≈0.5	1.030	1.68
B	8		6.15	0.145		1.048	

UNCLASSIFIED

Security Classification

DOCUMENT CONTROL DATA - R & D

(Security classification of title, body of abstract and indexing annotation must be entered when the overall report is classified)

1. ORIGINATING ACTIVITY (Corporate author)	2a. REPORT SECURITY CLASSIFICATION
Arnold Engineering Development Center ARO, Inc., Operating Contractor Arnold Air Force Station, Tennessee 37389	UNCLASSIFIED
	2b. GROUP N/A

3. REPORT TITLE

MEASUREMENTS AND CORRELATIONS OF TRANSITION REYNOLDS NUMBERS ON SHARP SLENDER CONES AT HIGH SPEEDS

4. DESCRIPTIVE NOTES (Type of report and inclusive dates)

Final Report July 30 to September 26, 1968

5. AUTHOR(S) (First name, middle initial, last name)

S. R. Pate, ARO, Inc.

6. REPORT DATE	7a. TOTAL NO. OF PAGES	7b. NO. OF REFS
December 1969	53	39

8a. CONTRACT OR GRANT NO.	9a. ORIGINATOR'S REPORT NUMBER(S)
F40600-69-C-0001 b. PROJECT NO. 8953 c. Task 03 d. Program Element 62201F	AEDC-TR-69-172 9b. OTHER REPORT NO(S) (Any other numbers that may be assigned this report) N/A

10. DISTRIBUTION STATEMENT

This document has been approved for public release and sale; its distribution is unlimited.

11 SUPPLEMENTARY NOTES	12. SPONSORING MILITARY ACTIVITY
Available in DDC.	Arnold Engineering Development Center, Arnold Air Force Station, Tennessee 37389

13. ABSTRACT

An experimental investigation of laminar boundary-layer transition on a sharp, 10-deg total-angle, insulated cone at zero yaw was conducted in the AEDC-VKF 12- and 40-in. supersonic wind tunnels at free-stream Mach numbers from 3 to 6. This research was directed toward defining the relationship between the aerodynamic noise disturbances and boundary-layer transition Reynolds numbers $(Re_t)_\delta$ in high-speed wind tunnels and has extended previously published planar results to include axisymmetric models. A significant increase in $(Re_t)_\delta$ with increasing tunnel size (similar to the planar results) is shown to exist. Sharp cone transition Reynolds numbers from ten facilities (12- to 54-in.) for free-stream Mach numbers from 3 to 14 and a unit Reynolds number per inch range from 0.1×10^6 to 1.2×10^6 have been correlated using aerodynamic-noise-transition parameters. A quantitative correlation of the ratio between cone and planar $(Re_t)_\delta$ values has been developed which demonstrates a strong Mach number dependence and also indicates a variation with tunnel size and unit Reynolds number.

DD FORM 1 NOV 65 1473

UNCLASSIFIED

Security Classification

14. KEY WORDS	LINK A		LINK B		LINK C	
	ROLE	WT	ROLE	WT	ROLE	WT
conical bodies						
aerodynamic configurations						
supersonic flow						
hypersonic flow						
boundary layer transition						
aerodynamic noise						
Reynolds number						
laminar flow						
wind tunnels						

AFSC
Arnold AFS Tenn